Spring 2007

Age strengthening of gray cast iron: alloying effects and kinetics study

Thottathil Viswanathan Anish

Department:

AGE STRENGTHENING OF GRAY CAST IRON: ALLOYING EFFECTS AND KINETICS STUDY

by

THOTTATHIL VISWANATHAN ANISH

A THESIS

Presented to the Faculty of the Graduate School of the

UNIVERSITY OF MISSOURI-ROLLA

In Partial Fulfillment of the Requirements for the Degree

MASTER OF SCIENCE IN METALLURGICAL ENGINEERING

2007

Approved by

_____	_____
Dr. Von L Richards	Dr. Kent Peaslee

_____

Dr. Susan Murray

ABSTRACT

Age strengthening of gray cast iron has become a critical issue with metal casters trying to optimize their process for the closest conformance to properties. This necessitated more robust and precise methods to predict age strengthening. Most foundries use age strengthening behavior to cast at higher carbon equivalents to facilitate smaller gating systems. Also, it is well known in the casting industry that the tool life improves with aging. Hence these foundries require a model to predict aging behavior and accelerate the mechanism from days to hours. This research focuses on the methods of composition adjustments to control aging properties, creating a model to predict the aging behavior at different temperatures and understanding the mechanism of aging.

Effect of nitride formers Ti, Al and B on aging behavior was evaluated. The results indicated the strong effect of Ti and Al to suppress aging. The role of Ti was analyzed further to understand the thermodynamics of aging process. The results from this study showed a direct correlation of iron nitride formation and aging.

The kinetics of aging was studied by evaluating aging behavior at room and elevated temperatures (100°C, 182°C and 285°C). Tensile strength-temperature-time curves were described using Arrhenius and Avrami-Johnson-Mehl kinetics and an attempt was made to create a predictive model for age strengthening in gray iron and to explain the mechanism behind it. The activation energy for diffusion of nitrogen in gray cast iron at temperatures below 150^{o}C was found to be 60kJ/mol and at temperatures more than 200^{o}C was found to be 34kJ/mol.

ACKNOWLEDGMENTS

First and foremost, I would like to thank Dr. Von Richards for his guidance and support throughout my curriculum at the University of Missouri – Rolla. Not only has he given me the opportunity to excel in a graduate program, but he also gave me the opportunity to write papers, attend conferences, and meet with professionals of the industry.

I would like to thank my committee members, Dr. Kent Peaslee and Dr. Susan Murray, for their assistance in my master's program. I would like to express my sincere gratitude to Dr. David Van Aken and Dr. Scott Miller for their valuable time and expertise to help me. Also, my thanks go to Dr. Simon Lekakh for the sincere support throughout my research. Not only has he helped me on my research papers, but also when I was unable to find enough hands to pour iron. I wish to thank all the staff members at the University of Missouri – Rolla, but mostly Denise Eddings, Joyce Erkiletan and Paula Cochran who gave me terrific help in a lot of administrative and logistic aspects.

My sincere thanks go to the people who worked with me in the foundry over the last two years: Brandon Kruse, Darryl Webber, Siddharth Gupta, Hank Rawlins, Mangesh Vibhandik, Jared Teague and Ed Druschitz. Thanks to all the undergraduate research assistants who provided great cooperation during my research. I want to thank all of my friends here in Rolla.

This thesis is dedicated to my parents. Without them, I would not have been able to reach this achievement.

TABLE OF CONTENTS

LIST OF ILLUSTRATIONS

Figure Page

LIST OF TABLES

Table Page

1. INTRODUCTION

1.1. BACKGROUND

The age strengthening of gray cast iron was first reported by Ebner in 1963[1]. Later, Nicola and Richards (1999) demonstrated statistically that significant age strengthening occurs in most gray cast iron alloys[2]. The increase in tensile strength ranged from 3.3% to 13.5% in this work. The rate of increase follows an Avrami-Johnson-Mehl curve, so that much of the change occurs in the first few days. Also, during this phase of research the nitrogen in excess of the stoichometric amount to combine with *Ti* as titanium nitrides was found to be an important factor affecting the level of age strengthening. Nicola and Richards proposed that age strengthening was related to the interaction of nitrogen with dislocations. The diffusivity of nitrogen in iron is significant at room temperature to facilitate these mechanisms[3].

In Phase II of this study, Richards et al (2000) verified the effect of nitrogen as a strength enhancer and that the presence of a strong nitride former (such as Ti) can reduce the strengthening effect in iron, but did not fully eliminate the aging[4]. The possibilities of precipitation of nitrides in the solid state and nitrogen in interstitial interaction with dislocations have been mentioned by Leslie (1981). Leslie (1981) also noted the development of substitutional-interstitial defect clusters, similar to those formed in steel. The main substitutional atoms considered were Mn, Cr, Si, and Mo, although V, Ti and Al can form similar clusters. These clusters interact with dislocations producing strengthening, the magnitude of which is less compared to age strengthening due to precipitation processes. Nicola *et al* (2000) indicated the presence of iron nitride and/or carbo-nitride were critical for aging. The presence of titanium did not appear to enhance or retard the age strengthening provided that nitrogen is in excess of that required for a stoichometric titanium nitride compound.

It is important to note that improvements in machinability occur concurrently with the age strengthening of gray iron. Various machining parameters were studied by Edington *et al*. (2002), and the results showed a sigmoidal relationship with the time of aging (Figure 1.1)[5]. Also in the same year, a neutron scattering study was conducted to determine the mechanism underlying aging. The scattering data revealed a resolved peak for the nitrogen-rich gray iron sample at 28 days. This peak corresponded to a particle with a diameter of 2-4nm or an ordered array of particles with interparticle spacing of 3.7nm. This size is similar in magnitude to the iron nitride clusters described by Edmonds and Honeycombe in 1978[6]. However, Edington et al did not have enough data to establish that aging is related to such a precipitation of particles because only one of the samples showed a peak in the scattering data. Edington et al (2002) also reported the role of free nitrogen in age strengthening . The age strengthening increased with an increase in free nitrogen. Free nitrogen can be defined as the amount of nitrogen available in the iron which has not formed any nitrides or carbonitrides. It is also important to note that this free nitrogen cannot necessary be soluble in iron because the solubility limit of nitrogen is limited by temperature and other alloy additions especially C and Si. The dissolved nitrogen measured for commercial malleable and nodular iron by Uda et al in 1974 was in the 80-90ppm range. Any excess free nitrogen that is beyond the solubility limit escapes as nitrogen gas or cause porosity in the castings. In this research, we consider dissolved nitrogen as free nitrogen since the nitrogen added was within the solubility limit of the iron. Therefore, total nitrogen can be defined as,

$$N_{Total} = N_{Free} + N_{Nitrides/carbonitride} \qquad (1.1)$$

In 2003, through differential scanning calorimetry, Richards *et al* established the strengthening phenomenon as a precipitation process which is reasonable in light of the Avrami-Johnson-Mehl transformation kinetics[7]. Differential scanning calorimetry studies (see Figure 1.2) revealed two significant exothermic reactions in fully aged gray iron: one at 250°C and the other at 530°C. At 250°C, metastable $Fe_{16}N_2$ *(α")* transforms to stable Fe_4N *(γ').* The second transformation (at 530^{o}C) is the ternary eutectoid transformation. Furthermore, the high temperature exothermic peak may be considered as the ternary

eutectoid transformation *(α-Fe + Fe3C + γ' → γ-Fe)* at 465°C. Also in this study, it was reported that hardness increased with time. All the reported results are consistent with an aging phenomenon associated with free nitrogen in the iron.

The background on age-strengthening of gray cast iron shows that the previous researchers were uncertain of the exact mechanism behind aging behavior. Previous work points towards the role of fine iron nitride precipitation behind the aging process. But, there was no information on a direct correlation of these with aging. Although work was done to establish accelerated aging, the kinetics of such a precipitation reaction was not studied in detail. This work focuses on explaining the mechanism behind aging by studying the thermodynamics of nitride precipitation and studying the kinetics of the same.

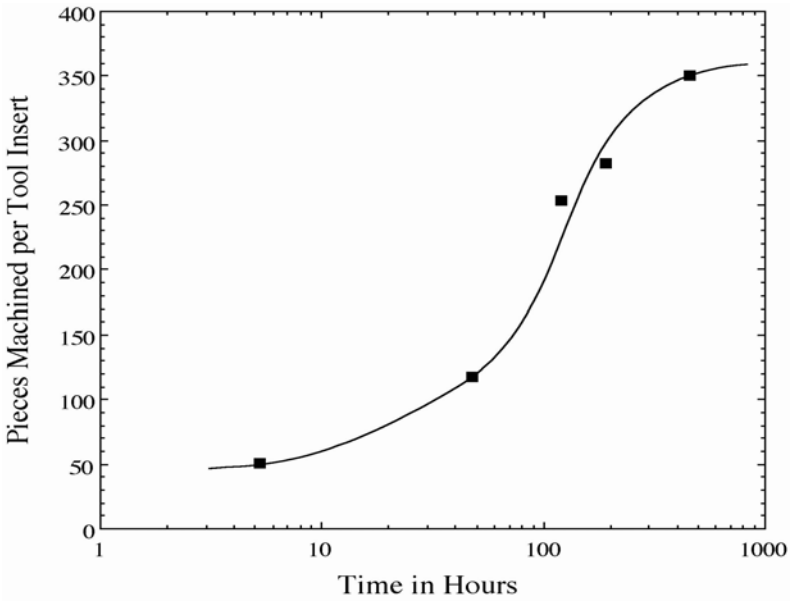

Figure 1.1. Effect of aging on machinability

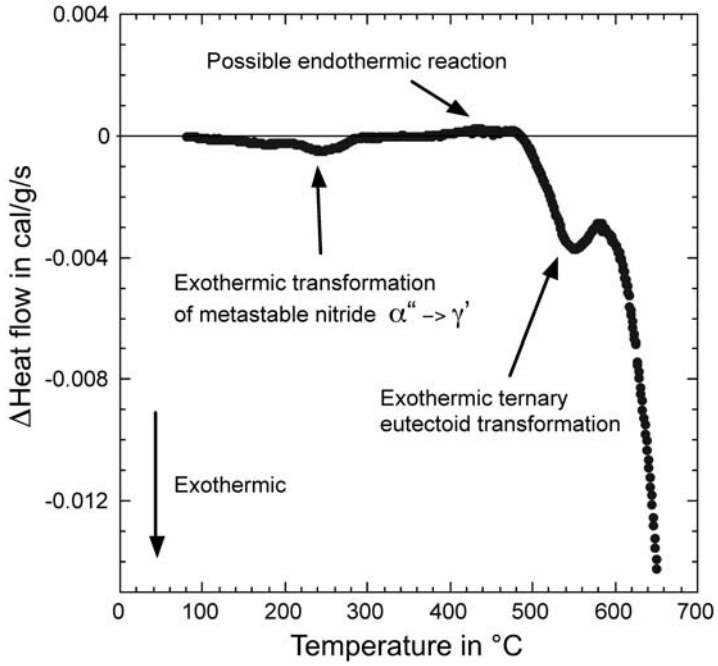

Figure 1.2. Differential scanning calorimetry results showing a difference curve generated by running a high nitrogen specimen in the reference cell and a non-aging specimen in the sample cell[7]

1.2. LITERATURE REVIEW

Although, there is limited work on age strengthening in the cast iron field, the research in certain aluminum alloys, copper alloys and steels is more exhaustive. Hence, to explain the age strengthening behavior in cast irons, it is necessary to understand the aging process described in these alloys.

1.2.1 Aging process. S. H. Avner has described aging behavior in non-ferrous alloys in detail[8]. According to Avner, an alloy, which is in a quenched state is a super saturated solid solution and is unstable. The excess solute tends to come out of the solution. Precipitation is accelerated by an increase in temperature and refrigeration retards this process. At temperatures below -50^{o}F, the process is delayed for extended periods. In the early theory of aging process, it was thought that the excess phase comes out of the solution as fine submicroscopic particles which interfere with the movement along slip planes, increasing strength. Later studies indicate that aging is not due merely to the

presence of precipitate. It is due to both the uniform distribution of finely dispersed sub-microscopic precipitates and the distortion of lattice structure by those particles before they coarsen. It is not clear to the researchers on how the precipitates harden the matrix or solvent lattice. The most important theory of such strengthening is the coherent lattice theory. After quenching of an alloy, it is in a super saturated condition, with the solute atoms distributed at random lattice structures. During an incubation period, the excess solute atoms tend to migrate to certain crystallographic planes, forming clusters. During aging, these clusters form an intermediate crystal structure, maintaining coherency with the lattice structure of the matrix. The excess phase will have different lattice parameters from those of the solvent, and as a result of coherency, there will be considerable distortion of matrix. It is this distortion that interferes with the movement of the dislocations, resulting in an increase in strength. Eventually the equilibrium phase is formed with its own lattice structure, leading to a loss in coherency with the matrix and lower distortions. The strength decreases and the alloy is "over aged". This kind of aging behavior is noted in Aluminum 2014 and certain Cu-Be alloys.

Aging behavior in steels is reported by Leslie. Fe-0.02%N quenched from 500^{o}C showed age strengthening at 25, 60 and 100^{o}C. At 100^{o}C, the magnitude of strength increase was less due to larger precipitates and greater inter-particle spacing. It was reported that at all three temperatures the precipitates formed were $Fe_{16}N_{2.}$

Leslie also reports the interactions between substitutional solute atoms and interstitials. The main substitutional atoms considered are Mn, Cr, Si, Mo, V, Ti and Al. These elements were known to hold C and N in close associations, as indicated by internal friction. The resulting substitutional interstitial dipoles can interact strongly with dislocations over a greatly expanded temperature range as compared to interstitials acting alone. These strengthening effects were referred as interaction solid solution strengthening by J. D. Baird et al (1972)[9].

Edmonds and Honeycombe (1978) provided a review of quench aging studies in Fe-N alloys that indicates a three-stage precipitation process beginning with the formation of

interstitial-atom clusters, followed by nucleation of metastable α"- $Fe_{16}N_2$, and ending with equilibrium γ'-Fe_4N. Precipitation of α"- $Fe_{16}N_2$ can be nucleated homogeneously at low temperatures and high nitrogen supersaturations or heterogeneously on dislocations at higher temperatures and low nitrogen supersaturations. At temperatures above 200°C, the metastable α"- $Fe_{16}N_2$ is replaced by the ordered γ'-Fe_4N.

1.2.2. Iron nitride precipitation. Malinov et al in 2001 showed that the equilibrium phases of Fe-N below 860K are α (super saturated ferrite), γ'(Fe_4N) and ε–Fe_2N[10]. The same authors also established that the interpretation for the formation of α" ($Fe_{16}N_2$) at lower temperature are that the α" phase develops as a precursor for α not only from ferrite and martensite, but also upon transformation of ε and γ' or the α" phase develops as an equilibrium phase below 440K. Figure 1.3 shows the Fe-N system.

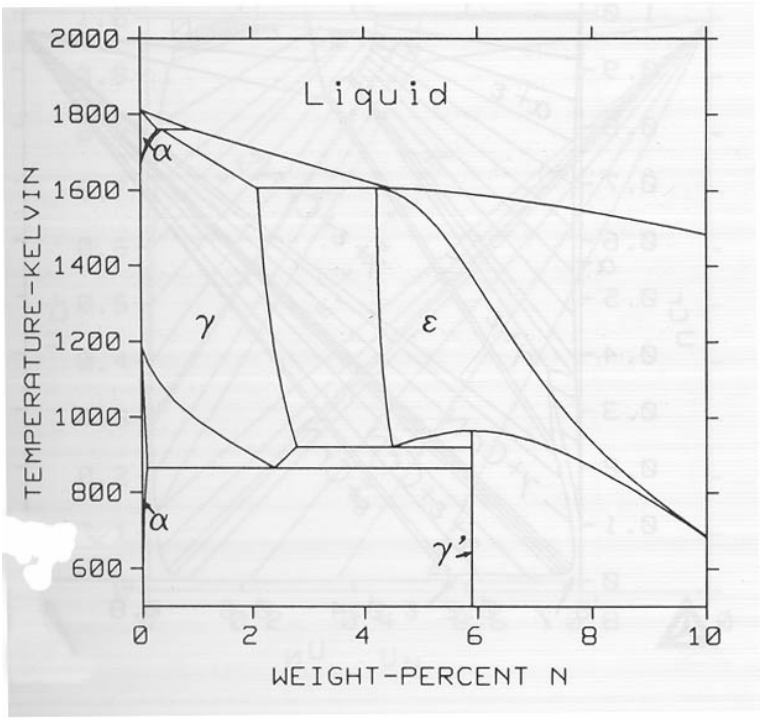

Figure 1.3. Fe-N system (Karin Frisk, 1987)[11]

Burgess (1968) also speculated the precipitation process as the reason for age hardening in ferritic malleable iron[12]. His conclusion was that aging occurs by the precipitation of carbides and/or nitrides from solid solution. He further adds that the effect of aging on mechanical properties depends primarily on the tangling of dislocations around

precipitated particles which acts as stress raisers. The distribution of precipitates played an important role. This distribution is in turn dependant on temperature. At high temperature it is present in the grain boundaries while at lower temperatures it occurs in the matrix also.

1.2.3. Nitride formers. Wada and Pehlke (1973) studied the effect of alloying elements on the graphitization in malleable and nodular cast irons[13]. Nitride forming elements such as aluminum, boron, titanium and zirconium accelerate graphitization in certain cases and retard graphitization in other cases. This is due to the characteristic behavior of nitrogen in iron with nitrogen getters. Nitrogen retards graphitization. When nitrogen is present with a nitrogen getter, they combine to form a stable nitride and precipitate from the matrix. Hence they have very less effect on graphitization. Most nitrogen getters have a retarding effect on graphitization. Hence the optimum would be the correct amount of nitrogen getters to nullify the nitrogen. If the concentration of nitrogen getters is higher, it leads to lesser graphitization. Also, they have pointed out that the nitride precipitates enhance the kinetics of graphitization by acting as nuclei. These authors consolidated solubility products of various nitrides (in gamma iron) from previous research papers:

<u>Al + N → AlN</u>

$$\text{Log } (\%Al)(\%N) = -\frac{7.184}{T} + 1.786$$

At $954^{o}C$, $(\%Al)(\%N) = 8.5 \times 10^{-5}$

<u>B + N → BN</u>

$$\text{Log } (\%B)(\%N) = -\frac{13970}{T} + 5.24$$

At $954^{o}C$, $(\%B)(\%N) = 7.2 \times 10^{-7}$

<u>Ti + N → TiN</u>

$$\text{Log } (\%Ti)(\%N) = -\frac{14400}{T} + 4.94$$

For malleable iron at $954^{o}C$ → $(\%Ti)(\%N) = 2.1 \times 10^{-4}$

For nodular iron at 954 Deg C → (%Ti)(%N) = 1.5×10^{-4}
These values are higher than that in Gamma Iron at 954 Deg C.

The total nitrogen content in Ti-bearing iron alloys increase mainly due to the formation of titanium nitride or carbonitride. These authors could identify TiN and TiC using x-ray diffraction analysis but were unable to identify Ti(CN). These authors studied the stabilities of TiN and TiC and reported that thermodynamically TiN is more stable than TiC.

Robert J. Glodowski (1981) reported on the various nitride formers used to eliminate nitrogen in wire drawn steels[14]. Nitride formers considered in this paper were Al, Nb, Ti, V and B. Of these, only V and Ti effectively reduce N. Nb is relatively ineffective because of its affinity towards carbon. AlN formation was found to be very sluggish as reported by F. G. Wilson and T. Gladman (1988)[15]. Nitrogen reduction by B was not confirmed in this paper.

R. W. Fountain and J. Chipman in 1962 studied the four phase equilibrium between austenite, BN, Fe_2B and gas[16]. They reported that the activity coefficient of nitrogen (in austenite) is decreased by boron. For a steel containing 0.004 wt% N, an available B content of 0.003 wt % above that combined as B_2O_3 should be sufficient to reduce the nitrogen below 0.001 wt %.

Evans, E. R., (1969) studied the interaction between nitrogen and aluminum in gray cast iron[17]. It was concluded that as the aluminum content in the iron is increased the effect of nitrogen is decreased. If the aluminum content is more than twice that of nitrogen in iron there will not be a significant increase in strength caused by nitrogen. Another noticeable finding is that iron of lower nitrogen and aluminum showed lesser strength that those with higher nitrogen contents and were neutralized by aluminum.

1.2.4. Solubility of nitrogen in cast irons. Uda et al. (1974) did a study to determine the solubility of nitrogen in cast iron[18]. They determined the solubility of nitrogen in a series

of Fe-C-Si alloys and commercial iron alloys over a temperature range 1287-1760^{o}C. Their studies show that C and Si reduce the solubility of nitrogen. They reported that there was a very small increase in solubility of nitrogen with increase of temperature. For Fe -2.82%C-1.94%Si, the temperature dependency of nitrogen solubility can be written as,

$$\text{Log (wt \% N)}_{\text{1 atm pressure}} = -\frac{1355}{T} - 1.096$$

The variation in solubility due to C and Si was mainly due to the effect of interaction parameters on the activity coefficient of nitrogen.

2. EXPERIMENTAL PROCEDURE

2.1. EXPERIMENTAL DESIGN

2.1.1. Alloying effects study. For determining the effects of alloying elements on age strengthening behavior, a design of experiments (DOE) approach was used. A combination of compositions of Ti, B, Al and N was developed based on a factorial model, the compositions and ranges were based on a survey of the participating foundry co-sponsors. The minimum value for the composition of titanium was kept at 0.01 wt% to represent actual foundry alloys. The matrix of compositions for the 16 DOE heats is shown in Table 2.1 and the base iron aim composition (for a class 30 gray iron) is shown in Table 2.2.

Table 2.1. Design matrix for 16 heats (ALAP= As Low As Possible)

#Heat	Alloying Components, weight %				Comment
	N	B	Al	Ti	
1	0.010	0.0015	0.015	0.01	
2	0.010	0.0015	0.015	0.04	maximum
3	0.010	0.0015	ALAP*	0.01	
4	0.010	0.0015	ALAP	0.04	
5	0.010	ALAP	0.015	0.01	
6	0.010	ALAP	0.015	0.04	
7	0.010	ALAP	ALAP	0.01	
8	0.010	ALAP	ALAP	0.04	
9	ALAP	0.0015	0.015	0.01	
10	ALAP	0.0015	0.015	0.04	

11	ALAP	0.0015	ALAP	0.01	
12	ALAP	0.0015	ALAP	0.04	
13	ALAP	ALAP	0.015	0.01	
14	ALAP	ALAP	0.015	0.04	
15	ALAP	ALAP	ALAP	0.01	minimum
16	ALAP	ALAP	ALAP	0.04	

Table 2.2. Base composition to achieve a nominally class 30 gray cast iron, weight %

Element	**Wt%**
C	3.4
S	0.06
Si	2.1
Mn	0.45
P	0.03
Cu	0.35
Cr	0.08

Based on the results from this matrix (Table 2.1), another set of experiments was designed to evaluate the role of titanium in thermodynamics of age strengthening in gray cast iron. The combination of titanium and nitrogen compositions was based on a monotonic model in which titanium was varied at four different compositions for two levels of nitrogen (Table 2.3), using the target base iron composition as shown in Table 2.2.

Table 2.3. Design matrix for eight heats to establish titanium-nitrogen effect

#Heat	*Alloying Components, weight %*	
	N	*Ti*
1	nominal	0.000
2	nominal	0.015
3	nominal	0.030
4	nominal	0.050
5	elevated	0.000
6	elevated	0.015
7	elevated	0.030
8	elevated	0.050

2.1.2. Kinetics study. The experimental conditions were designed based on published experimental data (Richards and Nicola, 2001) and the kinetics based on Johnson Mehl-Avrami kinetics. A generalized form of the Johnson-Mehl equation is shown as eq. (2.1)

$$V_f = 1 - \exp\left(\frac{-\pi}{3} J^r G^s t^{r+s}\right) \qquad (2.1)$$

where V_f is the fraction transformed, J is the nucleation rate, G is the growth rate, t is the transformation time and r and s are exponents related to nucleation and growth respectively. The Avrami equation (2.2) has also been used to describe phase transformations. Here the equation is written in a fashion such that the reaction rate constant k will always have units of reciprocal time.

$$V_f = 1 - \exp\left(-(kt)^n\right) \tag{2.2}$$

The rate constant k is defined by the following relationship:

$$k = k_0 \exp\left(\frac{-Q}{RT}\right) \tag{2.3}$$

where R is the gas constant, T is the absolute temperature, k_0 is an attempt frequency and Q is the activation energy. If k_0, Q and the time exponent n, are constant over a range of temperatures, then the reaction is said to be isokinetic in that temperature range.

The previously published results by Nicola et al (2001) and Edington et al (2002) showed that the age-strengthening effect was at a maximum after 15 days at room temperature aging, after 10 hours at 182°C and after 3 hours at 285°C[19,5]. A time exponent of 4 was chosen for the solid state precipitation transformation as mentioned in Cahn and Haasen (1983), which assumes a constant nucleation rate (r=1) and a 3-D growth of the precipitate (s=3)[20]. A value of JG^3 was determined for each temperature and the time (t) required to complete a particular fraction ($V_f(t)$) of the reaction was calculated. Figure 2.1 shows the calculated aging curves for room temperature, 182°C, and 285°C and these results were used to plan the age-hardening time interval for the cast iron used in this study. In addition, one set of bars was aged for longer periods of time to determine if the iron could be over-aged with a subsequent loss of strength. The extended time was 11 hours at 285°C, 28 hours at 182°C, 37 hours at 100°C and 48 days at room temperature. The test parameters are shown in Table 2.4. The procedure of randomizing the samples will be described below.

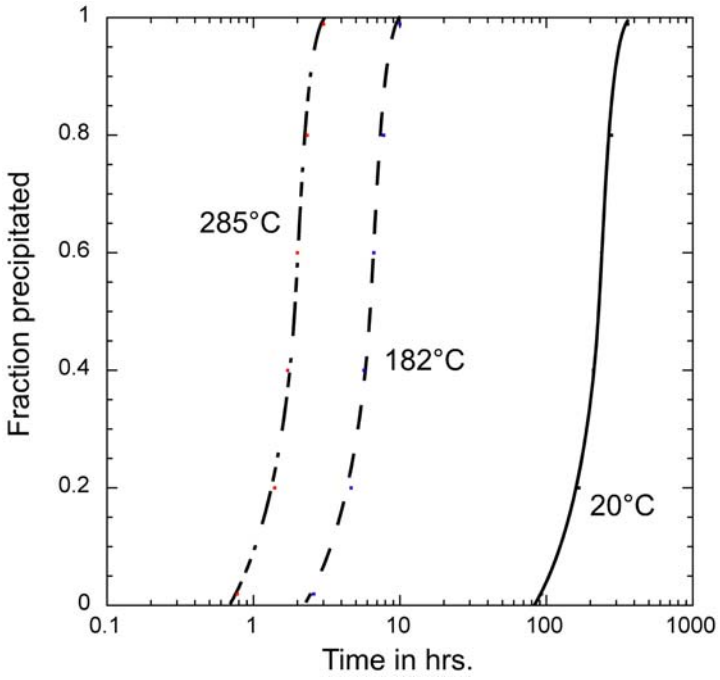

Figure 2.1. Forecast of aging kinetics by using Avrami-Johnson-Mehl equation

Table 2.4. Heat treatment time and temperature parameters

Temperature, °C	Aging time (hr)	Sample #		Temperature, °C	Aging time (hr)	Sample #		Temperature, °C	Aging time (hr)	Sample #	
Base	0	1	A	100	18.5	8	A	285	0.75	44	B
		23	A			6	A			49	A
		5	B			17	A			35	A
		26	A			48	B			43	A
		13	A			52	A			11	A
Base	0	16	A	100	37	46	B	285	1.5	21	B
		37	B			42	A			46	A
		12	B			9	B			2	B
		50	B			38	B			26	B
		16	B			29	B			25	B
Room T	4 day	18	B	100	27	39	A	285	2.5	29	A
		28	A			48	A			5	A
		50	A			41	A			2	A
		22	B			34	B			28	B
		20	A			9	A			1	B
Room T	6 day	45	B	182	4	18	A	285	5	14	B
		6	B			51	B			19	A
		4	B			14	A			52	B
		27	B			36	A			41	B
		31	B			7	A			4	A
Room T	9 day	38	A	182	8	10	B	285	11	20	B
		47	A			47	B			7	B
		19	B			17	B			11	B
		15	A			24	B			22	A
		40	B			24	A			32	B
Room T	15 day	21	A	182	12	35	B				
		44	A			3	A				
		45	A			39	B				
		33	B			23	B				
		13	B			33	A				
Room T	19 day	8	B	182	18	42	B				
		25	A			15	B				
		43	B			3	B				
Room T	25 day	34	A			31	A				
		30	B			10	A				
		49	B	182	28	27	A				
Room T	46 day	32	A			30	A				
		36	B			40	A				
		37	A			12	A				
						51	A				

2.2. MELTING PROCEDURE AND SAMPLE PREPARATION

2.2.1. Alloying effects study. 24 heats (16 heats from Table 2.1 and 8 heats from Table 2.3) of nominal class 30 gray iron (composition given in Table 2.2) with different levels of alloying elements have been poured. Each heat consisted of six molds having two vertically oriented test bars. The casting process is designed as per ASTM A48 standards with the exception that a filtered (ceramic foam) mold is used which is a typical industrial practice.

The composition of the base cast iron was achieved by melting pure induction iron bars (Table 2.5) in a 100-pound capacity induction furnace under an argon protective atmosphere by adding carbon raiser (99.97%C, 0.016%S, 9.75 ppm hydrogen, 36.3 ppm nitrogen and 59.3 ppm oxygen), Fe75Si, copper, FeCr, FeP and FeMn as solid charge to achieve the base composition in Table 2.2.

Table 2.5. Concentration of elements (weight %) in high purity iron bars

C	0.004
Si	0.01
Cu	0.01
N	0.004
Mn	0.07
Ni	0.02
Al	0.005
Ti	0.005
P	0.006
Cr	0.01
Sn	0.01
S	0.007
Mo	0.01
O	0.025
Fe	99.8

Ti was added as Fe - 75%Ti alloy wrapped in steel foil and plunged into the melt at a temperature of 1520^{o}C. In heats having low nitrogen, manganese was added as low carbon Fe - 82%Mn and plunged into the melt before tapping. The nitrogen in heats with elevated concentrations was added by using Fe-75%Mn-5%N. Tapping temperature was 1520$\pm$10^{o}C and inoculant (Superseed$^{®}$- 75%Si, 0.76%Sr, 0.17%Al, 0.03%Ca) was added to the preheated pouring ladle at the base of the tap stream. The pouring was done from the preheated ladle at a temperature of 1450^{o}C. The test bars were mold cooled for 15

minutes after which the bars were shaken out, allowed to cool in air for 40 minutes, cooled in water (from about 200^{o}C), and then placed on dry ice.

The test bars produced were machined at room temperature under coolant flow in conformance to ASTM A48 and SAE J431 using a CNC lathe. The time consumed for machining a bar was approximately seven minutes. Each mold has two vertically separated cast bars. Of the two sets of bars from each mold, one lot was stored in dry ice between each processing step until tested. That set of bars was machined and tested within a day while the other set from the same pour was allowed to age completely for 30 days at room temperature. The total room temperature exposure for the first set of bars (day 0) was typically 1.5 hours.

The heat labeled as "2" in Table 2.1 was attempted twice – once producing nitrogen content that was too low (less that 0.007) and once producing titanium content that was too low (less that 0.002). Therefore those heats with their actual analysis in the database as heats H02 and H002 were included and proceeded to analyze the data by regression correlations.

For chemical analysis, two chill samples were poured, one before and one after pouring the molds. The samples were analyzed in an arc spectrometer for Si, Cr, Mn, Ti, Al, P, and Cu. The results were then verified with another arc spectrometer. Nitrogen was analyzed using a LECO inert gas fusion analyzer. Carbon and sulfur were analyzed using a LECO carbon-sulfur combustion analyzer.

2.2.2. Kinetics study. Test bars were poured in one of the participating foundries. The casting process and melt recipe of the participating foundry was followed with the exception that the nitrogen level in the iron was raised from 60ppm to 70-81ppm by ladle addition of ferromanganese with nitrogen *(Fe75%Mn5%N)* to enhance age strengthening. Two chill samples were poured, one before and one after pouring the molds. The samples were analyzed in an arc spectrometer for Si, Cr, Mn, Ti, Al, P, and Cu. The results were verified with two other arc spectrometers. Nitrogen was analyzed using a LECO TC500

inert gas fusion analyzer. Carbon and sulfur were analyzed using a Leco carbon-sulfur combustion analyzer. Fifty molds having pressed ceramic filter and two vertically oriented test bars were poured. The temperature of the melt in the ladle at the beginning of pour was 1468°C and at the end of pouring was 1366°C. The castings were cooled for 20 minutes in the mold before shake out, air-cooled for 25 minutes to a temperature less than 120°C, and quenched in water for 5 minutes. The castings were numbered chronologically, and the two bars from each mold were designated as A and B and placed in dry ice. Sets with five bars each were grouped using a statistically randomized distribution. The test bars produced were machined at room temperature under coolant flow in conformance to ASTM A48 and SAE J431 using a CNC lathe. The time consumed for machining a bar was approximately 7 minutes. After machining, the test bars were immediately placed in dry ice again.

2.2.2.1. Artificial aging. A convection oven with an internal air recirculating fan was used for the artificial aging heat treatments. In addition to the oven temperature controller, the temperature of the samples was verified using a dummy test bar with an axial hole drilled to the center of the gage length. With this test arrangement, the aging time was recorded from the time the temperature inside the bar reached ± 5°C of the required aging temperature. The variation of temperature during the holding time was ± 1°C.

2.3. TESTING

Prior to mechanical testing, each bar was stabilized to room temperature in a water bath. Tensile tests were performed using an MTS Model 312.31 test frame with a 100 kN servohydraulic actuator and equipped with an Instron 8800 digital control and data acquisition system. Button-ended test specimens were held on the tapered shoulders in fully articulated box grips. Brinell hardness indentations were measured using an optical microscope equipped with a digital camera and a computer using a Scion Image

Analyzer. The calculated uncertainties in the reported measurements were based upon one sample standard deviation.

3. RESULTS

3.1. EFFECT OF ALLOYS

Table 3.1 lists the heats that have been completed from the matrix in Table 2.1. The data also show the average ultimate tensile strength for day 1 and for day 20, the difference in the averages, and the standard deviation of the data set for each day. H6 appears to be a bit of an anomaly where the apparent decrease between day one and day twenty is on the order of the standard deviation. This suggests there was some error in the experiment and was removed from analysis.

Table 3.1. Results summary – 16 heats (compositions - weight %)

Heat no:	%N	%B	%Al	%Ti	Day1 UTS, MPa	Day 1 Std Dev	Day 20 UTS, MPa	Day 20 Std Dev	Change in Avg. Strength (Mpa)
H 02	0.0069	0.0021	0.017	0.015	259.06	15.83	262	14.65	2.94
H 002	0.0091	0.0019	0.02	0.002	280.2	4.72	289.47	2.66	9.27
H 015	0.0068	0.0087	0.006	0.016	285	6.1	289.16	5.91	4.17
H 7	0.0096	0.0009	0.007	0.005	290.7	6.18	299.79	14.08	9.08
H 8	0.0093	0.0008	0.006	0.01	275.03	3.5	285.79	3.03	10.76
H 3	0.0085	0.0021	0.005	0.002	262.22	5.37	271.01	2.14	8.79
H 5	0.0091	0.002	0.006	0.011	286	4.39	291.5	12.71	5.5
H4	0.0098	0.0009	0.006	0.01	273.5	3.86	288.5	3.46	15
H 6	0.0091	0.0008	0.019	0.041	227.62	3.69	221.74	4.86	-5.88
H 13	0.0063	0.0009	0.021	0.009	273.33	9.42	273.65	8.01	0.33
H 11	0.0051	0.0019	0.004	0.006	217.78	3.32	223.9	9.98	6.12
H 12	0.0056	0.002	0.005	0.025	223.42	5.64	228.16	5.92	4.74
H 10	0.006	0.0018	0.016	0.034	237.32	4.25	240.78	4.71	3.46
H 9	0.0066	0.0019	0.017	0.004	300.15	2.78	299.35	15.85	-0.8
H 16	0.0053	0.0006	0.005	0.006	273.82	3.16	283.33	3.98	9.51
H 14	0.0051	0.0005	0.012	0.013	290.81	1.46	295.35	2.81	4.54
H 01	0.0089	0.0018	0.002	0.0053	312.77	8.46	328.98	3.97	16.21

A student's t-test was done on the two sets of data from each heat to verify the confidence level of aging. In this data one can see that some heats exhibited age-strengthening and some did not. Heats H002, H7, H8, H3, H4, H16, H14, and H01 showed age strengthening with 99 percent or higher confidence. Heat H6, where strength

decreased by 6MPa during aging, was clearly not age strengthening and we can say with greater than ninety percent confidence that H9 and H13 were not age strengthening and with 61 percent confidence that H02 was not age strengthening. Therefore the experiment has been successful in suppressing age strengthening and inducing age strengthening by varying the content of nitrogen, boron, aluminum and titanium in the same base alloy. Detailed composition data are shown in Appendix A.

Table 3.2 lists the heats that have been completed for evaluating the effect of titanium and nitrogen (Matrix given in Table 2.3). The data also show the N, Ti, average ultimate tensile strength for day 1 and for day 30 and the difference in the averages. HM-2 appears to be a bit of an anomaly as a result of low carbon equivalent. This data set was removed from analysis.

Table 3.2. Results summary – 8 heats (compositions - weight %)

Heat No:	N (%)	Ti (%)	UTS (Mpa) day 0	UTS (Mpa) day 30	Change in strength (Mpa)
HM-1	0.006	0.033	214.70	215.41	0.71
HM-2	0.005	0.019	325.22	321.82	-3.4
HM-3	0.006	0.034	246.30	247.83	1.83
HM-4	0.006	0.049	226.74	226.30	-0.44
HM-5	0.007	0.004	307.09	311.63	4.54
HM-6	0.008	0.026	278.66	282.14	3.49
HM-7	0.009	0.041	227.24	230.02	2.78
HM-8	0.009	0.063	214.90	215.27	0.10

The result of the influence of titanium at two levels of nitrogen (nominal and elevated) is shown in Figure 3.1. It can be interpreted from the figure that with increasing amount of titanium the age strengthening is reduced. The figure also shows that the absolute value of age strengthening is higher at elevated nitrogen experiments. At this nitrogen level, age strengthening was suppressed by a titanium content of 0.06-0.07%. It can also be noted that at the regular nitrogen level the age strengthening is suppressed with a titanium content of 0.03-0.04%

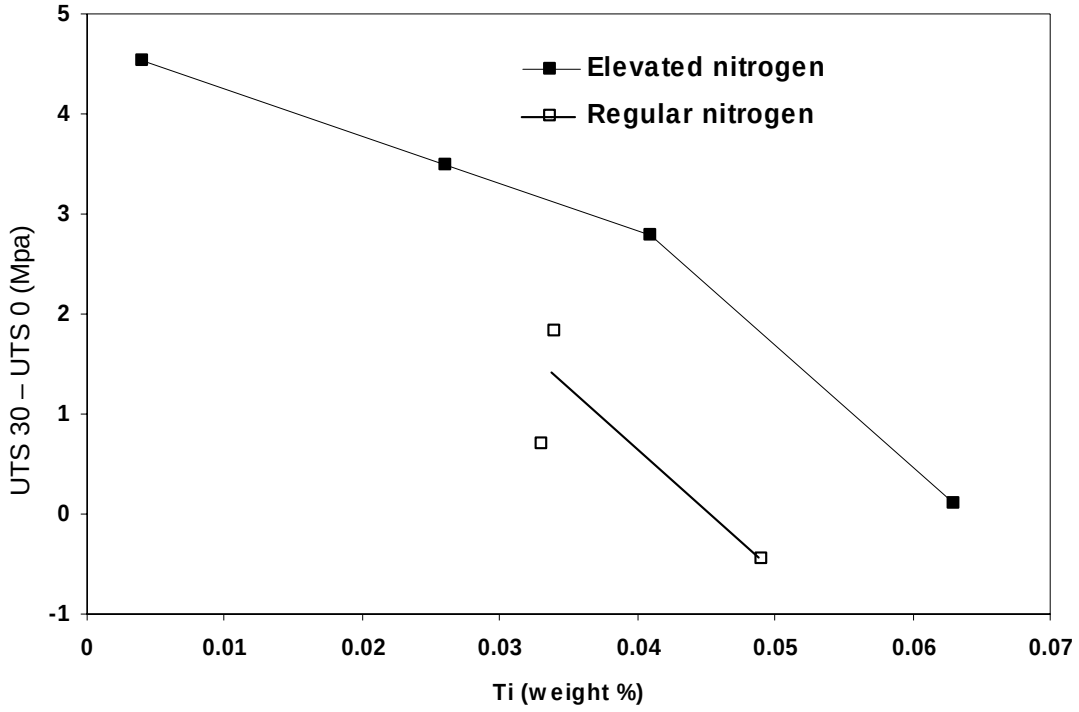

Figure 3.1. Change in tensile strength with titanium variations at two levels of nitrogen

3.2. KINETICS STUDY

Figure 3.2 shows tensile strength data with calculated averages and uncertainties for the aging studies. Brinell hardness measurements for these same irons are shown in Figure 3.3. Age strengthening was observed in both tensile strength and Brinell hardness measurements at all the temperatures studied. Natural aging was observed after 20 days and reached what appeared to be a terminal value after 24 days. Close examination of the tensile strength and hardness data for the room temperature and 100°C aged iron suggests a dip in the age-strengthening response. This dip occurs just prior to the onset of significant age strengthening at room temperature and 100°C. Although this dip is within the standard deviation, historical data of aging studies done by Edington et al and Richards et al suggests a similar event[5, 7] which can be attributed to some precipitation strengthening mechanism prior to age strengthening. Increasing the temperature accelerated the age strengthening process and decreased the peak aging times to 30-40 hours at 100 °C, 10-15 hours at 182°C, and finally, to only 4-6 hours at 285°C. Strength and hardness data for the elevated temperature aging studies show a continuous increase to a peak value. Increasing aging temperature from room temperature also increased the maximum value of tensile strength. An over-aging effect was also observed when the iron was aged at 182°C and 285°C where a loss in tensile strength was observed upon continued aging at these temperatures.

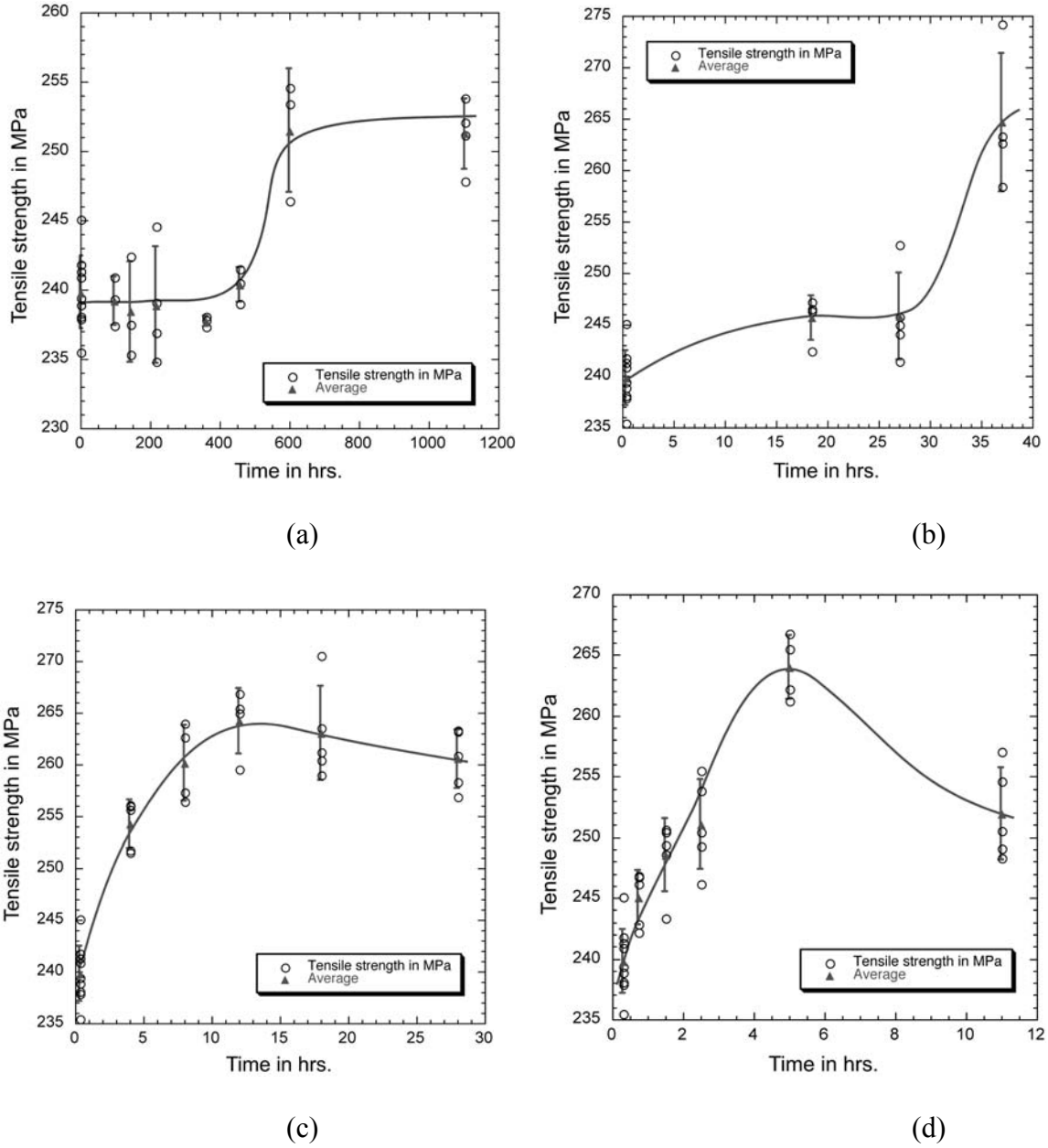

Figure 3.2. Tensile strength of iron during aging. (a) at room temperature (b) at 100°C (c) at 182°C and (d) at 285°C

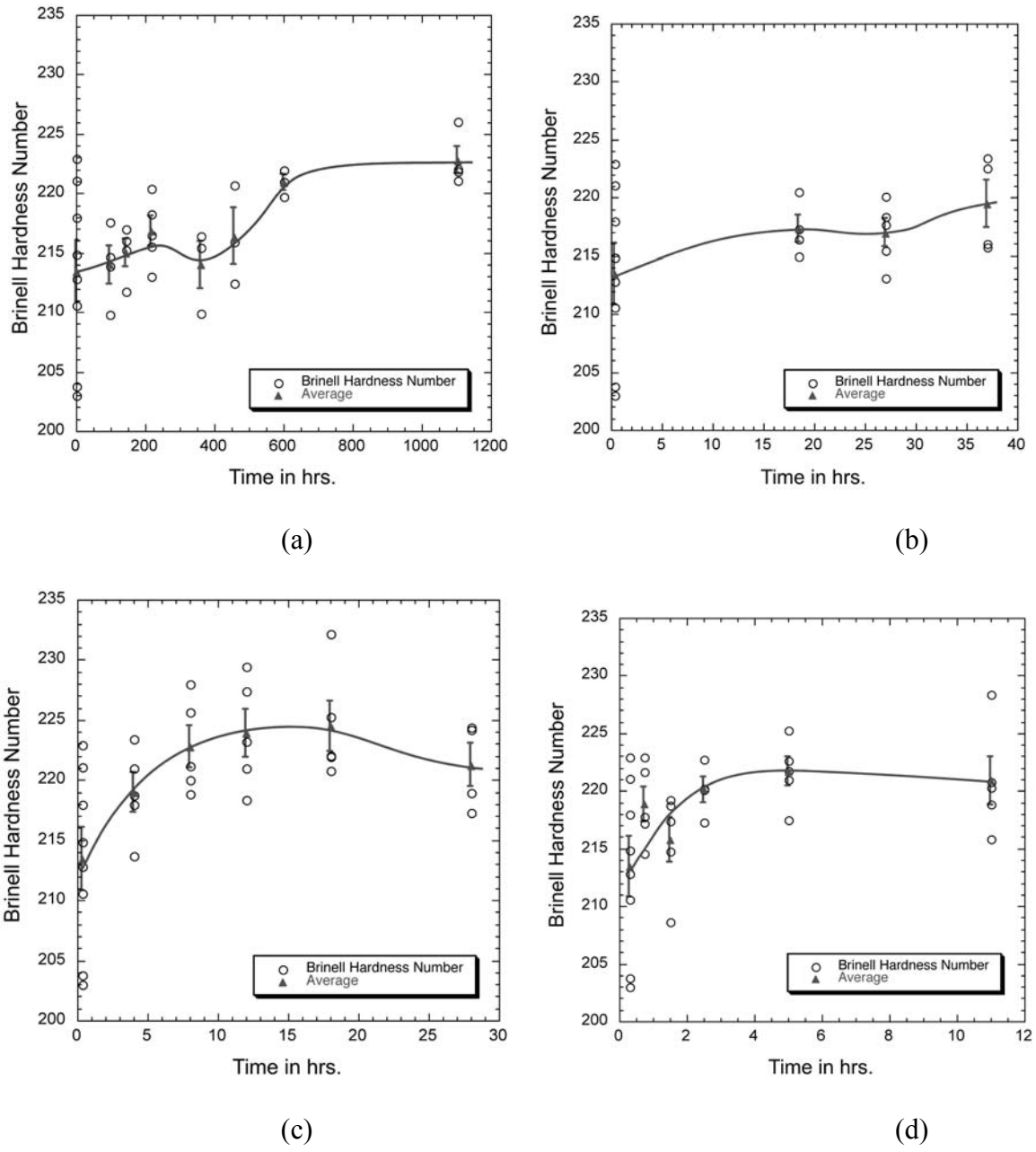

Figure 3.3. Brinell hardness of iron during aging. (a) at room temperature (b) at 100°C (c) at 182°C and (d) at 285°C

4. DISCUSSION OF RESULTS

4.1. EFFECT OF NITRIDE FORMING ALLOYS ON AGING BEHAVIOUR

In the first matrix of experiments (Table 2.1), the nitride formers Ti, Al and B were varied for two levels of nitrogen. Because the chemical variables used presented some difficulty in reproducible alloy recovery, the traditional ANOVA approach presented a problem. The ANOVA approach assumes only two values of each independent variable rather than in ranges as experienced in this study

Multiple variable regression correlation was used to assess the relative importance of variables in Table 2.1. It is important to note, as shown in Table 4.1, that the only compositional effect that increases age strengthening in this variable set appears to be nitrogen. Earlier work by Edington et al (2002) supports this, by indicating the importance of titanium to nitrogen ratio in production iron.

The multiple variable regression correlation approach was used to obtain an idea of the direction of influence and significance of the composition variables. The multiple variable regression results are shown in Table 4.1.

Table 4.1. Multiple variable regression model

Variable	Coefficient	P-Value
Nitrogen	+788	0.24
Aluminum	-324	0.07
Titanium	-173	0.09
Boron	-390	0.24
Constant	6.07	0.28

The overall equation suggested by the correlations is:

UTS_{20}-UTS_0 = 6.07+788*%N-324*%Al-173*%Ti-390*%B

Where "UTS_{20}-UTS_0" is the change in ultimate tensile strength in units of MPa for the initial aging of 20 days.

4.1.1. The effect of electropositive elements on nitrogen. The elements Ti, Al and B were selected for their tendency to react with nitrogen forming nitrides. The composition of each of these elements and their effect on the strength change was plotted and the correlation was studied.

The influence of nitrogen on age strengthening in this data set is shown in Figure 4.1. The presence of nitride formers, Ti, and Al reduced the amount of free nitrogen in the melt. The effect of B is not clear since the quantity involved is very small (0.0015 wt %) and the recovery was not consistent. Since the free nitrogen in the melt was significantly affected by these elements, the effect of total nitrogen in increasing age strengthening was weakened. This is supported by a very low R^2 of only 0.09. (R^2 is a statistical measure of how well a regression line approximates real data points. R^2 is a descriptive measure between zero and one, one being a perfect fit). Earlier work by Edington et al (2002) showed a better correlation between free nitrogen (N-0.33*Ti) and age strengthening, with an iron alloy in which aluminum and boron were controlled in a narrow range.

The enthalpy of formation of the nitrides of titanium, aluminum and boron in the temperature range from 1000^{o}K-1700^{o}K, the Fact-Sage database (Bale, et al, 2003) are:

Boron Nitride : -250KJ/mole
Aluminum Nitride : -329 KJ/mole
Titanium Nitride: -336$\pm$2KJ/mole

This data suggests that titanium nitride is the most stable nitride and hence titanium would be the most efficient element to remove free nitrogen from the melt, resulting in a reduction in age strengthening for the same total N. The enthalpy of formation of aluminum nitride is quite close to that of titanium nitride. The solution activity coefficient would have an effect on which nitride would form first. Boron should be less effective based on thermodynamic considerations. Titanium tends to react with nitrogen and carbon in the liquid state as is evident from typical titanium carbonitride morphology, while aluminum is known to form nitrides in the solid state in wrought steel technology (Leslie, 1983).

Figure 4.2 shows the effect of titanium on age strengthening. It shows that titanium in this data set tends to decrease age strengthening. Presence of other nitride formers, B and Al, can affect the formation of titanium nitride. This fact is supported by the low value of R^2 (0.32). The R^2 suggests that titanium level accounted for 32 percent of the variation in this dataset. Previous foundry data where other nitride formers were insignificant (Eddington, Richards and Nicola, 2002) show that there exists a better correlation between titanium and aging effect.

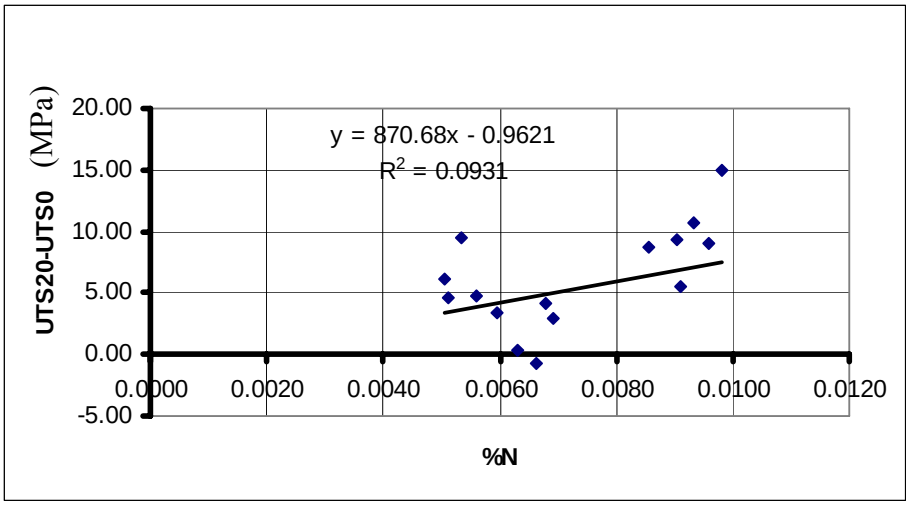

Figure 4.1. The effect of nitrogen on age strengthening: (Note that the vertical axis is the difference between the tensile strength within the first day and the tensile strength after 20 days natural aging.)

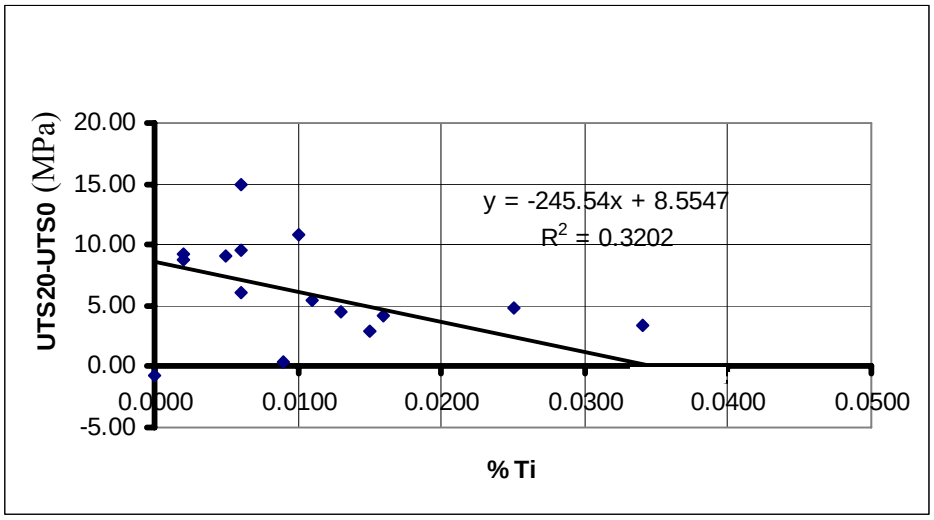

Figure 4.2. The effect of titanium on age strengthening: this is the strongest variable in terms of correlation coefficient and agrees with previous work using foundry irons

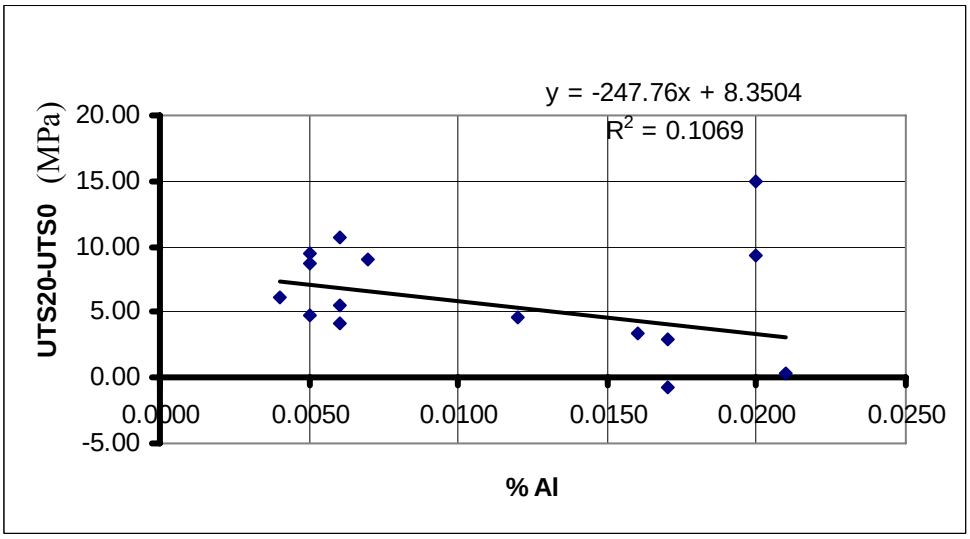

Figure 4.3. The effect of aluminum in this data set is to suppress age strengthening

The trend of aluminum on suppressing age strengthening, as indicated in Figure 4.3, is in agreement with anecdotal observations by some of the authors on production foundry irons that did not seem to exhibit age strengthening. Again the scatter in the data is considerably high (R^2 value of 0.11 indicates a low correlation) showing that other nitride

forming elements have affected the correlation between aluminum and aging properties. The titanium at high levels may override the aluminum effect.

A similar analysis using a linear statistical model for boron indicates a weakly suppressing effect for age strengthening. The effect of B could not be determined with any statistical significance because of the difficulty in recovering the very small alloying quantity and measuring boron level.

In terms of physical metallurgy, aluminum and titanium are relatively effective at removing interstitials from ferrite (carbon and nitrogen). Wada and Pehlke examined the Gibbs free energy of Ti-N and Ti-C phase and determined that Ti-N was more stable than Ti-C. Titanium carbo-nitrides are observable in gray iron microstructures with planar interfaces that reflect their crystal structure and suggest formation in contact with the liquid. If the coefficients in the multiple regression models (Table 4.1) are corrected for the atomic weight ratio between the titanium and nitrogen and aluminum and nitrogen, it is found that the corrected coefficients are more similar in magnitude, -623 for aluminum (in place of -324) and -524 for titanium (in place of -173) However, the boron coefficient becomes significantly smaller.

To study the effect of free nitrogen, the stability of nitrides needs to be considered. Since titanium nitride is more stable than aluminum nitride, in alloys that contain more of titanium than Al, the chances of formation of aluminum nitride is very small. Hence, for heats having Ti>0.01wt% in Table 3.1, the free nitrogen can be calculated based on atomic mass and 1:1 stoichoiometry as,

$$\% \text{ Free N} = \%\text{Total N} - 0.33\%\text{Ti} \qquad (4.1)$$

The effect of free nitrogen in high titanium heats on age strengthening is shown in Figure 4.4.

For heats having Ti<0.01wt% in Table 3.1, Free nitrogen can be calculated as

$$\% \text{ Free N} = \%\text{Total N} - 0.33\%\text{Ti} - 0.52\%\text{Al} \qquad (4.2)$$

The effect of free nitrogen in low titanium heats on age strengthening is shown in Figure 4.5.

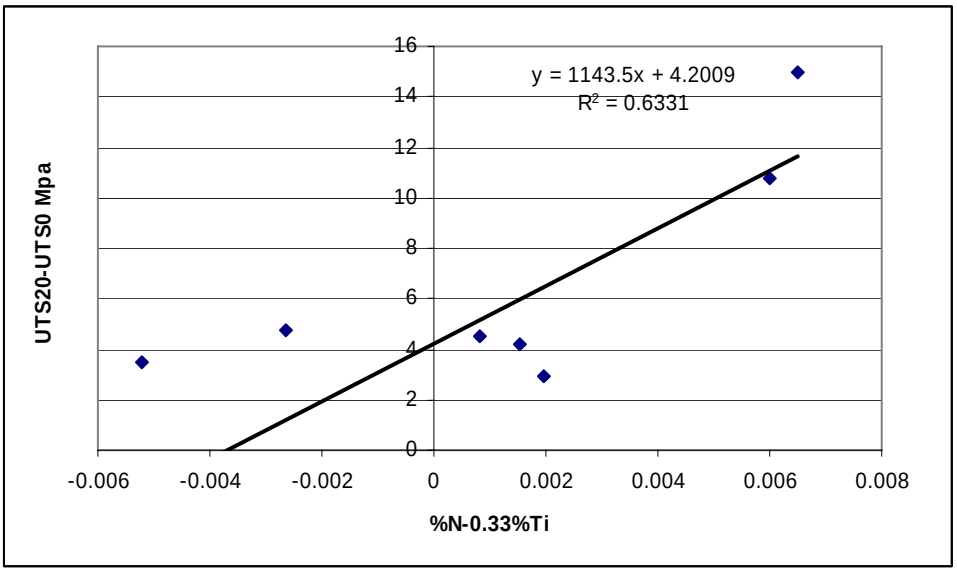

Figure 4.4. Estimate of free nitrogen in high titanium alloys as a controlling variable for age-strengthening

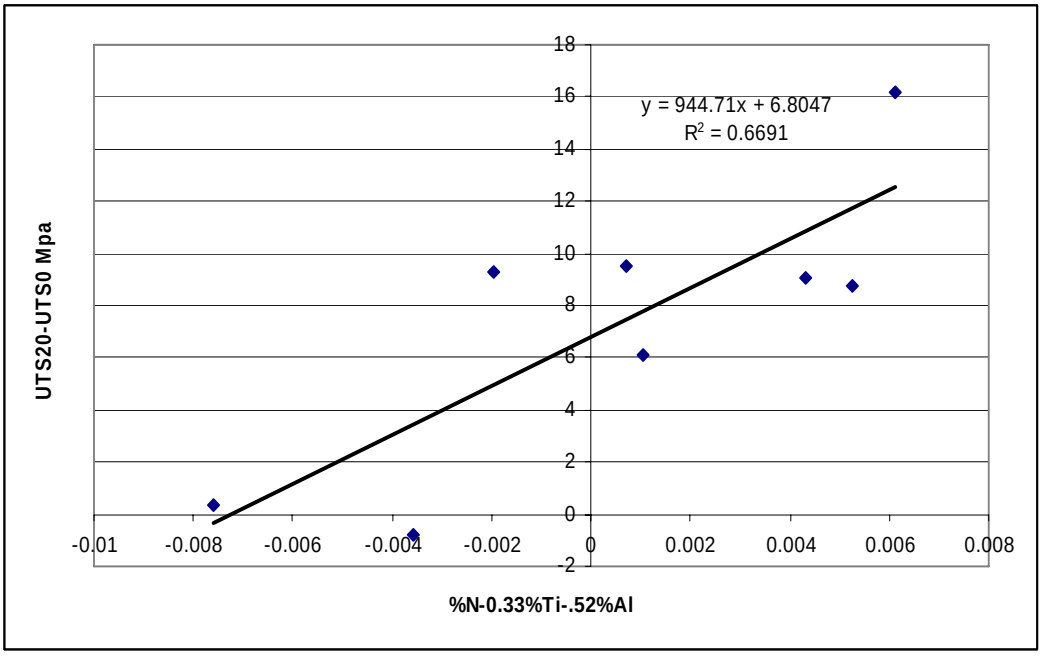

Figure 4.5. Estimate of free nitrogen in low titanium heats as a controlling variable for age-strengthening

Figures 4.4 and 4.5 indicate that free nitrogen improves age strengthening behavior. The R^2 values indicate that the correlation is strong. This result also supports earlier findings by Edington et al (2002).

A proposed age strengthening mechanism is that nitrogen and carbon in super saturated ferrite react with iron to form a precipitate. Titanium removes nitrogen from the iron during solidification and lowers the available nitrogen for solution in the ferrite. Aluminum may also remove some nitrogen during solidification and as the casting cools through the austenite temperature range forming aluminum nitride or carbo-nitrides. The net effect of titanium and aluminum reacting with nitrogen is to reduce the solubility of nitrogen in the ferrite and possibly the carbon solubility in ferrite. This leaves less nitrogen to react with iron in the aging process. From these 16 heats it was clear that both titanium and aluminum strongly reduce age strengthening.

But a serious limitation in this 16 heat matrix study was the co-existence of different nitride formers. Their interactions affected the correlation of a particular element with age strengthening behavior making it difficult to explain age strengthening based on a thermodynamic model. The second matrix of 8 heats (Table 2.3) concentrates on studying the effect of only titanium at two levels of N.

The multiple variable regression correlation approach was used to obtain an idea of the direction of influence and significance of the composition variables given in Table 2.3. The multiple variable regression results are shown in Table 4.2.

Table 4.2. Multiple variable regression model of the statistical effects of titanium and nitrogen

Variable	Coefficient	P-Value	Confidence
Nitrogen	704.4	0.0103	>95%
Titanium	-99.1	0.001	>99%
Constant	0.27	0.8182	18%

The overall equation suggested by this correlation is

$$\text{Change in UTS} = 0.267 + 704.4*N - 99.1*Ti$$

$$(R\text{-squared} = 95.15\%)$$

As expected, nitrogen has strong positive influence on age strengthening and titanium suppresses age strengthening which is in confirmation with earlier studies by Nicola et al (1999, 2000)[2,4].

Free nitrogen was calculated based on Equation (4.1). Figure 4.6 shows the relation between estimated free nitrogen and the change in strength upon aging. Aging effect increases with free nitrogen. The R^2 value of 0.87 shows that the result is in good agreement with earlier work by Edington et al (2002) and supports the result from the initial 16-Heat matrix.

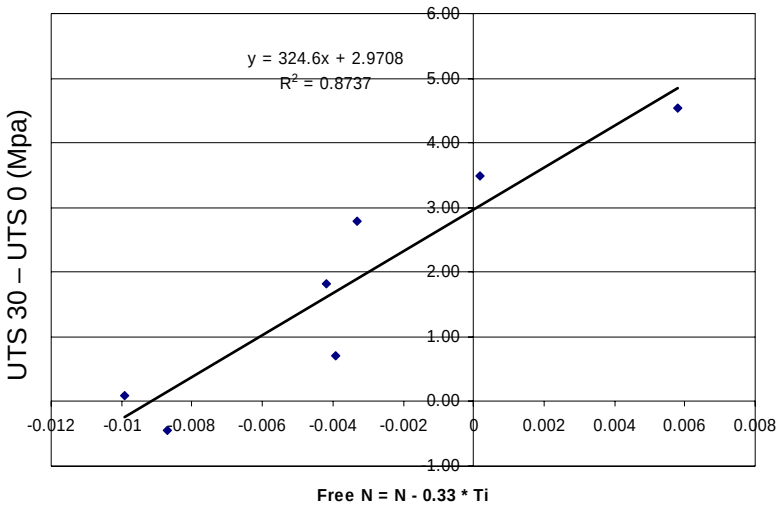

Figure 4.6. Effect of estimated free nitrogen on aging

4.1.2. Thermodynamics of age strengthening. Thermodynamic calculations were performed for understanding the interactions of controlled impurities of nitrogen and titanium in the iron melt as well as during solid phase transformation. Thermodynamic data also could be useful for evaluation of driving forces of iron aging which could also influence real process kinetics. The calculations were performed with FACTSAGE, software description of which could be found elsewhere (Bale, et al, 2003)[21,22]. Briefly, the computational method based on the Gibbs energy minimization of system contains the initial levels of base components (Fe-3.5%C-2%Si) with controlled impurities of nitrogen and titanium. The program identifies the most probable reactions and products which have the most negative Gibbs energy:

$$G = \sum_{\substack{ideal\\gas}} n_i\left(g_i^0 + RT\ln P_i\right) + \sum_{\substack{pure\\condensed\\phases}} n_i g_i^0 + \sum_{solutions} n_i\left(g_i^0 + RT\ln X_i + RT\ln\gamma_i\right)$$

Where:

n_i - moles;

P_i - gas partial pressure;

X_i - mole fractions;

v_i - activity coefficient;

g_i - standard molar Gibbs energy.

The FACTSAGE data base includes the thermodynamic properties of liquid iron solution, austenite, ferrite as well as special phases: iron and titanium nitrides and carbides (Fe_4N, TiN, Ti_2N, TiC, Ti(CN)). The influence of other components typically present in iron (C, Si) was evaluated using activity coefficients.

Results of the calculations are presented below as a function of titanium additions into iron (Fe-3.5%C-2%Si) with two levels of nitrogen (Figure 4.7). The low level had 0.004% nitrogen and the high level had 0.009% nitrogen that reflected the possible maximum and minimum concentrations in experimental conditions. The possible interactions in liquid iron near the solidification temperature of 1200°C are depicted in Figure 4.7. Pure iron dissolves free (not chemically bonded) nitrogen in solution. When the concentration of titanium is between 0.015% and 0.04%, the iron melt had some residual dissolved nitrogen and also chemically bonded nitrogen with titanium as a nitride phase. Above 0.04-0.05% Ti, practically all titanium has chemically bonded with nitrogen and the excess titanium formed carbides and carbonitrides. A point to note is that theoretical predictions showed no thermodynamic conditions for the formation of iron nitrides directly in the melt.

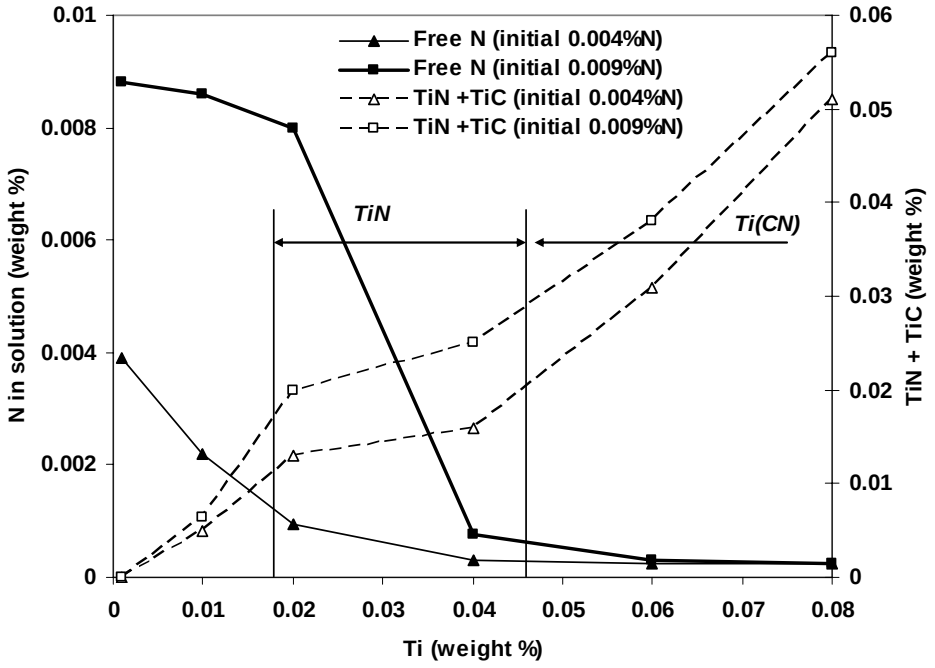

Figure 4.7. Interactions of titanium in iron melt with different initial concentrations of nitrogen

Iron solidification significantly change the thermodynamic conditions of nitrogen in solid iron solution and nitrogen activity depend on temperature and existing stable iron phases (γ- iron or α-iron). In pure iron alloys without any nitride formers, practically all nitrogen is in true solid solution in austenite as well as in ferrite at high temperatures. While the temperature decreases from approximately 400°C to room temperature, ferrite becomes supersaturated and nitrogen can precipitate as iron nitride (Figure 4.8). This is the main thermodynamic condition for natural iron aging. The real mechanism, which is explained later in this section, could include several intermediate stages. This is typical for solid phase transformations which require larger activation energy when compared to liquid melt conditions where atomic mobility is high. The age-strengthening effect could be in proportion to a degree of ferrite super-saturation and a volume of iron nitride according to the thermodynamic equilibrium with ferrite.

The volume of equilibrium iron nitride significantly depends on the nitrogen content in iron as well as the concentration of nitride-forming elements, in particular titanium,

which has a large affinity towards nitrogen. When the iron alloy contains titanium and nitrogen simultaneously, these elements react to form titanium nitride resulting in a lower amount of "free" nitrogen in the solid solution. This limits the formation of iron nitride at room temperature and consequently suppresses iron aging effect. The particular percentage of equilibrium iron nitride is important from practical point of view because this allows predicting age-strengthening effect. The thermodynamic conditions of titanium nitride formation from solid austenite solution become stronger with decreasing temperature. This is a well known fact which is often used for decreasing austenite grain size in specially heat treated low alloyed steels[3]. When austenite is transformed to ferrite, the dissolution of titanium and nitrogen continues to decrease, which thermodynamically promotet titanium nitride formation. The temperature range of super-saturation of ferrite lies from room temperature to 300°C and beyond this range the possibility of aging is limited according to thermodynamics. The experimental data confirmed these thermodynamical predictions.

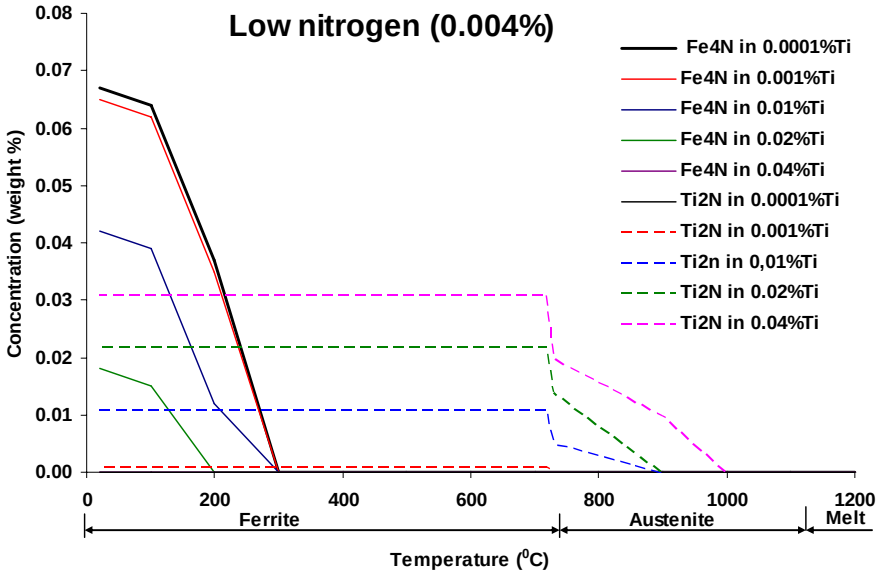

a)

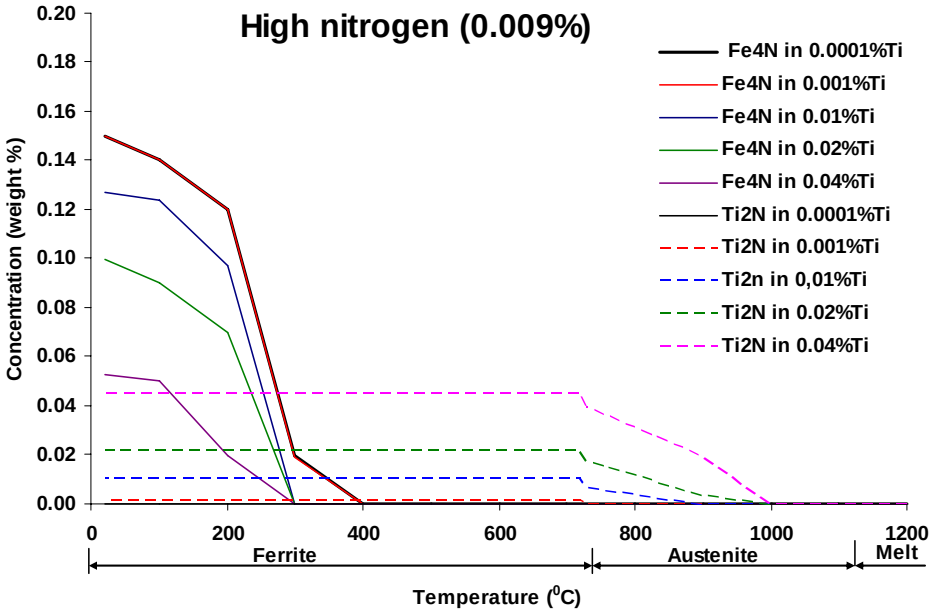

b)

Figure 4.8. Equilibrium of iron and titanium nitrides in solid irons with different initial nitrogen levels (a - 0.004%N and b - 0.009%N) as a function of temperature and titanium concentration

Three dimensional diagrams (Figure 4.9) shows the combined temperature and titanium content effect on "free" nitrogen in supersaturated ferrite and the possible percentage of iron nitride formation during the natural aging of gray iron. The figure 4.8 shows the combined effect at low and high nitrogen respectively. High nitrogen iron alloys have higher value of iron nitride and requires a higher concentration of titanium to suppress age strengthening.

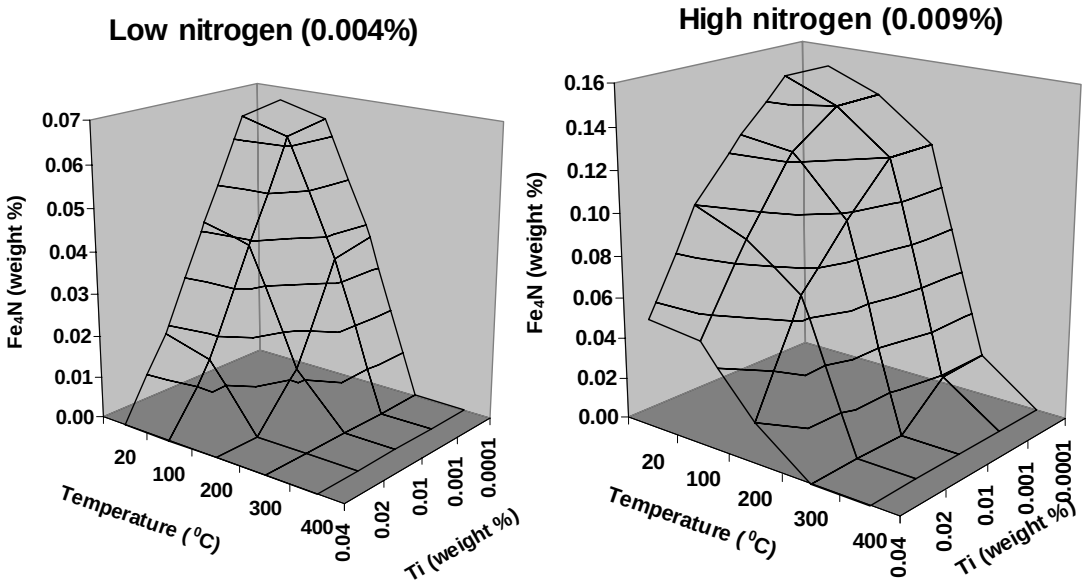

Figure 4.9. Combined influence of temperature and titanium of potential percentage of iron nitride formation during natural aging

The computed thermodynamical data of iron nitride formation in cast iron based on the compositions from Table 3.2 were compared to the experimentally measured age strengthening (Figure 4.10). The strengthening effect correlates to the computed percentage of potential iron nitride in iron. The suppressing of natural aging took place when the concentration of titanium exceeded 0.02% in heats with regular nitrogen levels, while in heats with elevated nitrogen, it occurred when titanium was higher than 0.06%.

Under these conditions, there are no possibilities for iron nitride formation according to the thermodynamical predictions. The thermodynamic modeling can also be used for more complicated industrial irons containing other impurities which have a potential for reacting with nitrogen.

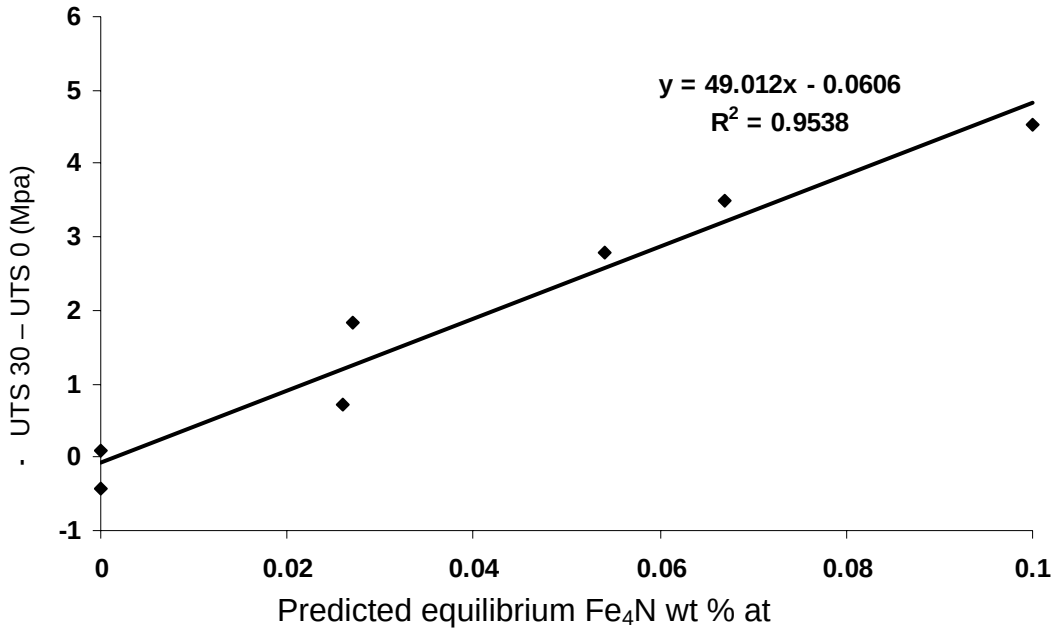

Figure 4.10. Comparison of experimentally measured age strengthening effect with predicted formation of iron nitride

4.1.3 SEM analysis. To support the formation of different nitride phases in iron and its effect on aging, a SEM (Scanning Electron Microscope) study was undertaken to observe the presence of these inclusions. For this study, the samples were chosen from Heat 6 of Table 3.1, because these samples also contained other nitride formers which correlate to the actual foundry practices. A low magnification EDS map was taken to get information on the location of titanium and aluminum inclusions (Figure 4.11). The blue region represents iron, the green region is oxygen, yellow region is aluminum and red region is

titanium. It can be seen from the figure that there are definite spots of red which have no correlation to the oxygen map which indicates the possibility of nitride inclusions. These locations were studied under larger magnification (Figure 4.12). The inclusions were mostly cube type with an average size of approximately 5 microns. These inclusions were analyzed using EDS to confirm the composition of titanium nitride (Figure 4.12).

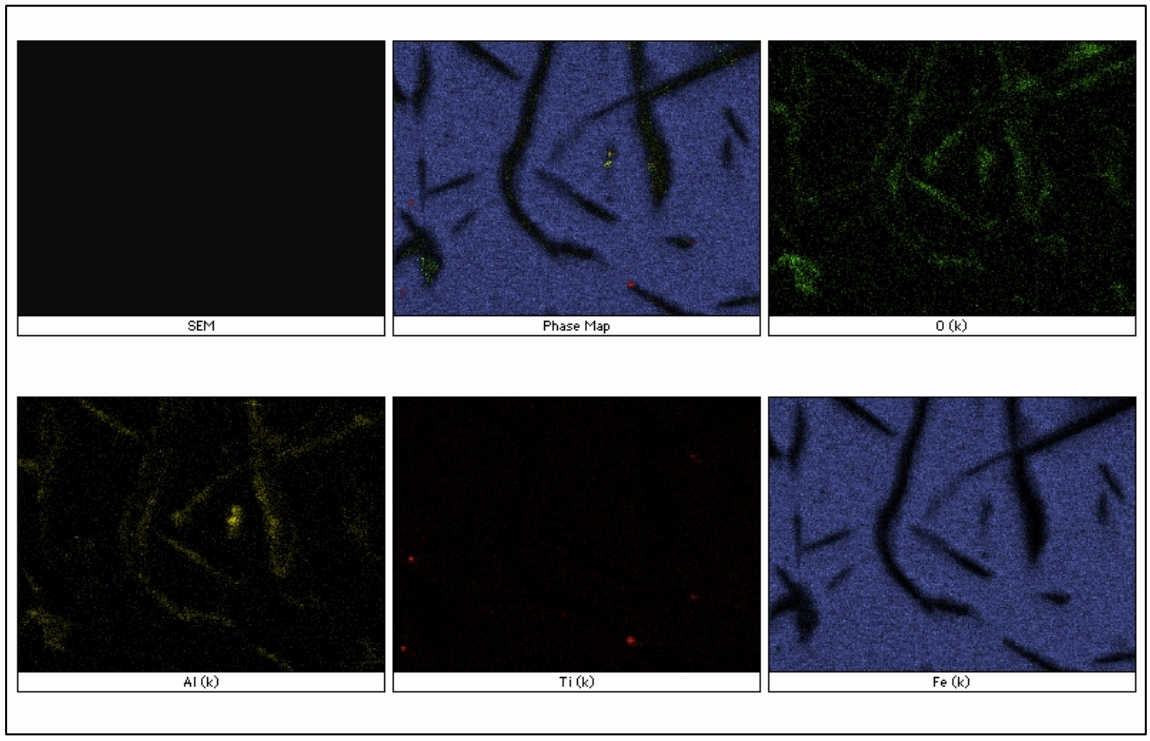

Figure 4.11. EDS map of sample from Heat 6 from Table 3.1

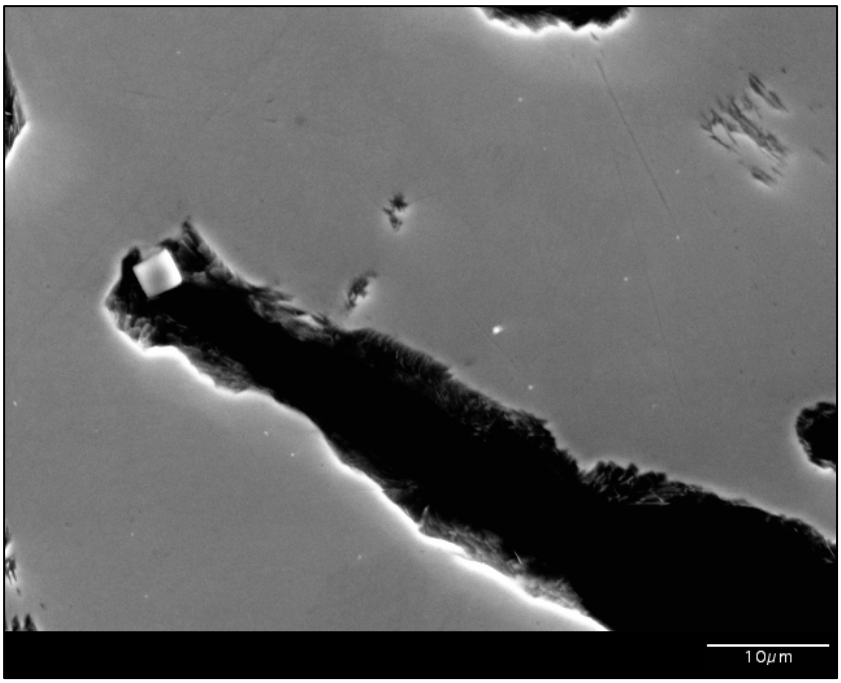

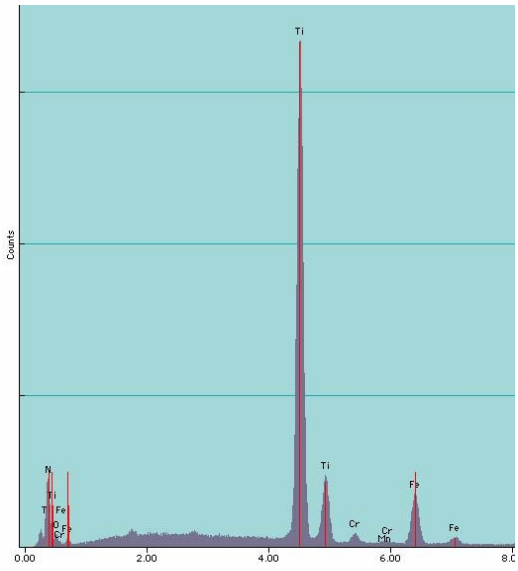

Quantitative Results for Spectrum2
Analysis: Bulk Method: Standardless
Acquired 17-Apr-2006, 15.0 KeV @10 eV/channel

Element	Weight %	Atomic %
N	1.98	6.30
O	2.73	7.63
Ti	74.07	68.99
Cr	2.17	1.86
Mn	0.30	0.24
Fe	18.75	14.98
Total	100.00	

Figure 4.12. TiN inclusion in Heat 6 of Table 6 and EDS spectra of the same

4.2. KINETICS OF AGE STRENGTHENING

Results in section 3.2 for elevated temperature aging (Figure 3.2.) shows that full natural aging was completed in 25 days, which is significantly longer than the 15 days observed in previous studies (Nicola *et al* 2001). The difference in aging kinetics could be explained by chemistry variations (see Table 4.3). The iron, which showed faster aging, had a higher concentration of free nitrogen and a lower manganese content. Manganese can significantly retard the nucleation of iron nitrides in steel (Enrietto *et al.* 1962) by forming a substitutional and interstitial complex in the α-Fe[23]. Thus, a combination of lower free nitrogen and higher manganese may have contributed to a slower room temperature age-hardening response in the current study. The Mn-N complexes are also known to interact with dislocations and produce strengthening. Thus, the loss in strength and hardness just prior to the onset of age strengthening may be related to the depletion of nitrogen from these Mn-N-dislocation complexes.

Table 4.3. Comparison of iron chemistry and aging time at room temperature

Parameters	Previous test (Richards, *et al*., 2001)	Current study
Manganese, wt.%	0.51	0.80-0.83
Nitrogen, wt.%	0.0094	0.007-0.008
Aluminum, wt.%	0.003	0.005
Titanium, wt.%	0.012	0.014
Boron, wt.%	0.002	0.008
Soluble interstitial, wt.% (N – 0.33Ti)	0.0054	.0028
Natural aging time, days	15	28

Measured strength data were converted to a fraction precipitated, V_f, using the following relationship between the peak strength, S_{max}, the initial strength at $t = 0$, S_{min}, and the strength measured during aging, $S(t)$:

$$1 - V_f = \frac{S_{\max} - S(t)}{S_{\max} - S_{\min}} \tag{4.3}$$

Base samples (the set of 10 tensile bars which was tested at minimum aging time) and the samples that over-aged were removed from the analyses using Avrami and Arrhenius equations. Hence, the chosen data consist of all data sets that would fall on the positive slope of the Strength-Time curves of Figure 3.2. The Avrami equation, Equation (2.2), was then used to evaluate the age strengthening kinetics of the iron (see Figure 4.13). Two distinct regimes are depicted in Figure 4.13, indicating that the age strengthening is not isokinetic over the temperature range investigated. At elevated temperatures (T>150°C), the time exponent, n, was determined to be 1.8 whereas the lower temperature data were fit by n=3.7. Rate constants were determined from Figure 4.13 where kt=1, which corresponds to an ordinate value of one in Figure 4.13.

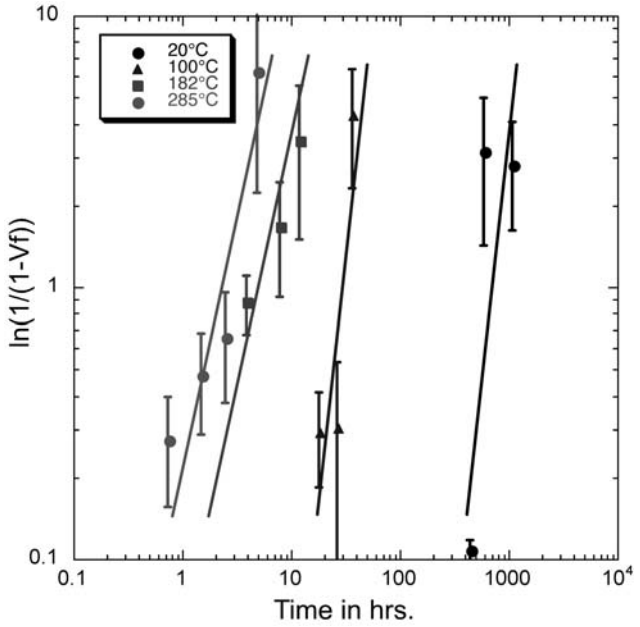

Figure 4.13. Age hardening data graphed assuming standard Avrami kinetics

An Arrhenius plot was constructed (see Figure 4.14) using the rate constants as determined above, with the abscissa as ln(k in hrs.$^{-1}$) versus the ordinate as reciprocal of the absolute temperature (1/T(K)). An activation energy of Q=17kJ/mole was determined for the 285 °C and 182 °C data whereas Q= 36kJ/mole was determined for the 100 °C and 20 °C data. Rasek (1983) reported an activation energy of 44kJ/mol for precipitation growth of nitrides in an Fe-N system over the temperature range of 50°C to 180°C[24]. It

should be noted that activation energies determined using the Avrami relationship require considerable interpretation before a relationship to the diffusing species controlling the reaction rate is established.

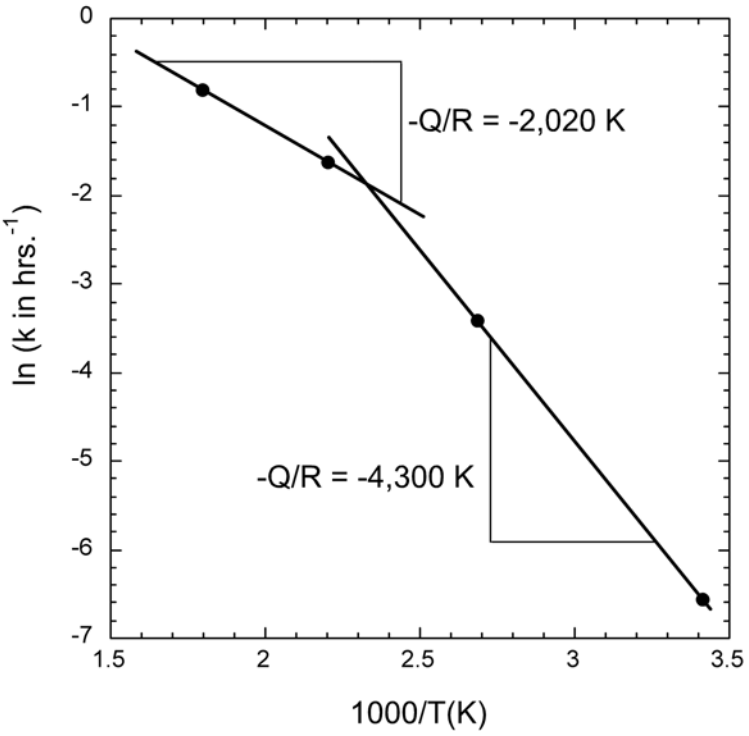

Figure 4.14. Arrhenius plot of iron aging kinetics

The activation energy, Q, may be written in terms of the activation energy for diffusion, q, the activation energy barrier to nucleation, ΔG^*, and the activation energy barrier to add an atom to the growing nucleus, $\Delta g^{\ddagger}$. Equation (4.4) is obtained by equating the exponential terms in the Johnson-Mehl equation (2.1) for nucleation and growth with the exponential term in the rate constant k in the Avrami equation (2.2).

$$Q = \frac{r}{n} N_a \left(\Delta G^* + \Delta g^{\ddagger} \right) + \frac{s}{2n} q \qquad (4.4)$$

The expression above is for a transformation where a single new phase grows according to the parabolic growth law, where the growth velocity, G, is proportional to the diffusivity to the power 1/2 ($D^{1/2}$). In evaluating the various activation energies of this study, the transformation was assumed to be well below the solvus temperature of the precipitate. Thus, ΔG^* will be on the order of 10^{-19} J/ nucleus. For interstitials, $\Delta g^{\ddagger}$ was assumed to be zero, because interstitials do not occupy a lattice position in the parent phase and may be transported along the core of dislocations at the interface. Activation energies for diffusion (q) were then calculated for the different regimes and time exponents. For temperatures below 150°C, the time exponent was measured as 3.7, indicating a decreasing nucleation rate (r = 0.7) and spherical growth (s = 3) of the nucleus. An activation energy of 60kJ/mole was calculated for volume diffusion using Equation (6). The accepted value for nitrogen diffusion in α-Fe as measured by Wert (1950) is 76.1 kJ/mole[25].

At temperatures above 200°C, iron nitrides are known to precipitate on dislocations and grow as discs with habit planes of $\{100\}_{\alpha\text{-Fe}}$ for α"- $Fe_{16}N_2$ or $\{210\}_{\alpha\text{-Fe}}$ for γ'-Fe_4N Edmonds and Honeycombe (1978). Thus, the nucleation could be considered as site saturated (r = 0) where all of the nuclei exist at the beginning of the transformation. If n=2 is assumed for the time exponent, which corresponds to the growth of a disc-shaped particle (s = 2), then a value of 34kJ/mole is calculated for the pipe diffusion of nitrogen along the dislocation core, which is approximately half the activation energy for lattice diffusion.

4.3. MECHANISM OF AGE STRENGTHENING

Edmonds and Honeycombe (1978) provided a review of quench aging studies in Fe-N alloys that indicates a three-stage precipitation process beginning with the formation of interstitial-atom clusters, followed by nucleation of α"- $Fe_{16}N_2$, and ending with equilibrium γ'-Fe_4N. Precipitation of α"- $Fe_{16}N_2$ can be nucleated homogeneously at low temperatures and high nitrogen supersaturations or heterogeneously on dislocations at higher temperatures and low nitrogen supersaturations. At temperatures above 200°C,

the metastable α"- $Fe_{16}N_2$ is replaced by the ordered γ'-Fe_4N. This paper proposes that the same sequence occurs during the age strengthening of gray irons. In this regard, the neutron scattering studies reported by Edington et al. (2002) support evidence of interstitial atom clusters in the order of 2-4nm that are spherical in shape, and the low temperature kinetic results (activation energy of 60kJ/mole for iron nitride precipitation) reported in the previous section support that conclusion where the time exponent (n=3.7) suggests an equiax-shaped precipitate. The rate of cluster formation also appears to be affected by manganese concentration where high manganese concentrations may retard cluster formation. Furthermore, the apparent dip in strength and hardness data prior to the onset of age strengthening may be a result of dissociation of nitrogen from N-Mn-dislocation complexes and the initial stages of nitrogen cluster formation. The strength of these clusters would be proportional to the cluster radius and the cluster volume fraction to the power of ½ ($r^{1/2}P_f^{1/2}$), which assumes that the cluster is sheared by a moving dislocation. At longer aging times, α"- $Fe_{16}N_2$ precipitates on dislocations and depletes the clusters via pipe diffusion along dislocation cores. It should be anticipated that α"-$Fe_{16}N_2$ precipitation may be more homogeneous in irons with higher nitrogen supersaturations than in those studied here. Aging temperatures of 182°C and 285°C are most likely above the solvus temperature of α"- $Fe_{16}N_2$ for the irons studied here, and heterogeneous precipitation of γ'-Fe_4N on dislocation would be anticipated. This conclusion is supported by the low value of activation energy and a time exponent that roughly agrees with the growth of a disk-shaped particle as expected for γ'-Fe_4N. Furthermore, the strength aging curves at 182°C and 285°C suggest a single precipitation event.

Modeling the low-temperature age-strengthening response in gray irons is complicated by the manganese effect; however, the results from this study suggest that irons can be formulated with low manganese and high nitrogen to obtain a quicker aging response. Heat treatment may also be an option and possibly less dependent upon the manganese content. The following relationship is based upon the 182°C and 285 °C aging kinetics observed in this study, where the time to peak age, t_{peak}, is calculated in hours and temperature, and T is the absolute temperature in Kelvin.

$$t_{peak} = 0.171 \exp \frac{2020}{T} \tag{4.4}$$

Peak aging times of 14.5 hours and 6.4 hours are predicted for the aging temperatures of 182°C and 285°C, respectively, using Equation (4.4). Complete understanding of age strengthening in gray irons will require further study and it should be cautioned that Equation (4.4) does not account for alloy chemistry, e.g., nitrogen and manganese, which may affect both the precipitate sequence and aging kinetics.

5. CONCLUSIONS

It can be concluded from the alloying effects experiment is that titanium and aluminum suppress age strengthening. The effect of free nitrogen was also verified. The thermodynamics of nitride precipitation reactions occurring during age strengthened explained the effect of titanium and nitrogen on aging. The experimentally measured values of age strengthening correlate to the potential equilibrium quantities of iron nitride at room temperature estimated by FACTSAGE.

The kinetics study revealed that the age-strengthening phenomenon in gray iron is not limited to a single mechanism at all temperatures and that over-aging is possible. Full strength can be achieved in as little as 4-6 hours at 285°C. Approximate activation energy values have been obtained that show the aging process is most likely associated with nitrogen clusters at low temperatures and nitride precipitation at elevated temperatures. Activation energy for diffusion of nitrogen in gray iron was found to be 34kJ/mole at temperatures below 150^{o}C and 60kJ/mole for temperatures above 200^{o}C. A predictive model for the time to peak age was formulated based upon the elevated temperature aging study and may be useful in planning accelerated aging processes at temperatures between 150°C and 300°C.

APPENDICES

APPENDIX A.

COMPOSITION EFFECTS ON AGE STRENGTHENING OF GRAY IRON

Composition Effects on Age Strengthening of Gray Iron

Von L. Richards, Thottathil V. Anish, Simon Lekakh, and David C. Van Aken
University of Missouri – Rolla, Rolla, MO
Wayne Nicola,
Consultant, Warsaw, IN

ABSTRACT

Due to the apparent influence of nitrogen solubility in ferrite on the age strengthening behavior of gray iron, a study was undertaken of the effects of nitrogen and elements that should interact strongly with it on the basis of thermodynamics. Those elements that were considered in addition to nitrogen were aluminum, titanium, and boron. This study used a designed experiment approach to study the effects of these elements in gray cast iron alloys that were synthesized from pure materials. Aging behavior was measured in terms of the change in strength for a fixed time interval at various combinations of the composition. Data suggests that for the range of compositions usually encountered, nitrogen has a strong influence on increasing the age-strengthening, aluminum and titanium have a strong influence on decreasing age-strengthening and the effect of boron was not as statistically significant in this study as titanium and aluminum. Titanium and aluminum were found to be the most effective at suppressing age-strengthening behavior.

Previous work on this subject by Nicola and Richards (1999) has demonstrated statistically that there is significant age strengthening in most gray cast iron alloys. The increase is in the range of 3.3 to a high of 13.5%. The same authors have demonstrated the machinability improvements with aging. The Temperature dependence and kinetics were also studied and established. Evidence of precipitate formation has been shown using neutron scattering methods. Differential thermal analysis studies have revealed two significant exothermic reactions in fully aged gray iron: one at 250^{o} C and the other at 530^{o} C. At 250^{o} C, transformation of metastable Fe-N to stable Fe-N happens and the second transformation is the ternary eutectoid transformation.

INTRODUCTION

This work is the result of AFS related research. The research is the continuation of previous work done by Nicola and Richards. They have proved statistically the existence of aging and the effects of nitrogen (1999, 2000). The strength increase kinetics follow an Avrami-Johnson-Mehl curve, so that much of the change occurs in the initial few days. In the early work (Phase II in 2000 – Richards, Van Aken and Nicola) from foundry A and B, where some castings aged

and others did not, nitrogen content in excess of that which could be taken out of solution by titanium was found to be the important factor. Their studies have indicated the presence of iron nitride and/or carbo-nitride forming as the mechanism for aging. The presence of titanium does not appear to enhance or retard the age strengthening provided nitrogen is in excess to that required for stoichiometric titanium nitride compound. Age strengthening is not observed when there is a large excess of titanium. Also, there is strong evidence that the gray iron aging process is a precipitation process. In Phase III (2001 Nicola and Richards) it was found that the aging process may be accelerated by elevating the temperatures to 180^{o} C. Improvements in machinability occur concurrently with the strengthening of gray Iron. Various machining parameters were studied by Richards, Nicola and Van Aken (2002) and the results show a similar Avrami-Johnson-Mehl relationship with the time of aging. Later, Richards, Nicola and Van Aken (2003) established the strengthening phenomenon as a precipitation process through differential thermal analysis and neutron scattering measurements, which is reasonable in light of the Avrami-Johnson-Mehl transformation kinetics.

The objective of this study was to evaluate the effects the minor alloying elements Al, B, N & Ti on the age strengthening process. The electropositive elements were chosen such that they are strong nitride formers in ferrous metallurgy.

EXPERIMENTAL PROCEDURE

DESIGN OF THE EXPERIMENT

A combination of compositions of Ti, B, Al and N to be added with the base iron was developed based on a factorial model. The compositions and ranges were determined based on input from the participating foundry co-sponsors. The matrix of compositions for the sixteen heats is given below in Table 1, and the base iron aim composition is shown in Table 2.

Table1. Design Matrix for 16 heats (ALAP = As Low As Possible).

#Heat	Alloying Components, weight %				Comment
	N	B	Al	Ti	
1	0.010	0.0015	0.015	0.01	
2	0.010	0.0015	0.015	0.04	maximum
3	0.010	0.0015	ALAP*	0.01	
4	0.010	0.0015	ALAP	0.04	
5	0.010	ALAP	0.015	0.01	
6	0.010	ALAP	0.015	0.04	
7	0.010	ALAP	ALAP	0.01	
8	0.010	ALAP	ALAP	0.04	
9	ALAP	0.0015	0.015	0.01	
10	ALAP	0.0015	0.015	0.04	
11	ALAP	0.0015	ALAP	0.01	
12	ALAP	0.0015	ALAP	0.04	
13	ALAP	ALAP	0.015	0.01	
14	ALAP	ALAP	0.015	0.04	
15	ALAP	ALAP	ALAP	0.01	minimum
16	ALAP	ALAP	ALAP	0.04	

Table 2. Base composition of cast iron, weight %

C	3.4
S	0.06
Si	2.1
Mn	0.45
P	0.03
Cu	0.35
Cr	0.08

CASTING PROCESS

Sixteen heats of nominal class 30 gray iron with different levels of alloying elements have been poured. Each heat consisted of six molds having two vertically poured test bars. The casting process is typical industrial practice with the exception that a filtered mold is used.

The composition of the base cast iron melted in 100-pound capacity induction furnace under argon protective atmosphere from high purity iron bars (Table 3) with addition of carbon raiser (99.97%C, 0.016%S, 9.75 ppm hydrogen, 36.3 ppm nitrogen and 59.3 ppm oxygen), Fe75Si, copper, FeCr, FeP and FeMn in solid charge.

Table 3. Concentration of elements (weight %) in high purity iron bars used as charge material

C	Si	Cu	N	Mn	Ni	Al	Ti	P	Cr	Sn	S	Mo	O	Fe
0.004	0.01	0.01	0.004	0.07	0.02	0.005	0.005	0.006	0.01	0.01	0.007	0.01	0.025	99.8

The alloys were added by plunging in iron foil packets at a temperature of 1520^{o}C. The nitrogen was added by substituting a nitrogen-containing ferromanganese. Tapping temperature was 1520$\pm$10^{o}C and inoculant was added to the pouring ladle at the base of the tap stream. The pouring was done from the preheated ladle at a temperature of 1450^{o}C.

The test bars are mold cooled for 15 minutes after which the bars are shaken out and allowed to cool in air for 40 minutes. Then the bars were cooled in water (from about 200^{o}C) and placed on dry ice.

Test bars produced were machined at room temperature under coolant flow in conformance to ASTM A48 & SAE J431 specifications using a CNC lathe. Of the two sets of bars from each mold, one lot was stored in dry ice between each processing step until tested. That set of bars was machined and tested within a day while the other set from the same pour was allowed to age for 20 days at room temperature. The total room temperature exposure for the first set of bars (day 0) was typically 1.5 hours. Gauge Length sections were polished with 80-grit abrasive cloth strips while still chucked in the lathe.

Seventeen heats were poured and tested. The heat labeled as "2" in Table 1 was attempted twice – once producing nitrogen content that was too low and once producing titanium content that was too low. Therefore we simply included those heats with their actual analysis in the database as heats H02 and H002 and proceeded to analyze the data by regression correlations.

CHEMICAL ANALYSIS

Two chill samples were poured, one before and one after pouring the molds. The samples were analyzed in an arc spectrometer for Si, Cr, Mn, Ti, Al, P, & Cu. The results are verified with two other arc spectrometers. Nitrogen was analyzed using an inert gas fusion analyzer. Carbon and sulfur was analyzed using a carbon-sulfur combustion analyzer. Boron has been analyzed to date with one of the spectrometers that routinely does boron. The archived samples are also being analyzed for boron by ICP mass spectrometer.

TESTING

Tensile tests were performed using a 27000 pound capacity computer-interfaced load frame using a fully articulated fixture with box grips riding on the tapered shoulders of the button ended specimens for self-alignment. Loading times where in the 29-35 second range.

Brinell hardness indentations were measured using an optical microscope equipped with a digital camera and a computer using Scion Image Analyzer.

RESULTS

The heats that have been completed are listed in Table 4. The data also shows the average ultimate tensile strength for day one and for day 20, the difference in the averages and the standard deviation of the data set for each day. H6 appears to be a bit of an anomaly where the apparent decrease between day one and day twenty is on the order of the standard deviation. This suggests an alloy which decreases in strength with time.

Table 4. Results Summary

%N	%B	%Al	%Ti	Day1 UTS, MPa	Standard Deviation	Day 20 UTS, MPa	Standard Deviation	Change in Avg. Strength	Heat number
0.0069	0.0021	0.0170	0.0150	259.06	15.83	262.00	14.65	2.94	H 02
0.0091	0.0019	0.0200	0.0020	280.20	4.72	289.47	2.66	9.27	H 002
0.0068	0.0087	0.0060	0.0160	285.00	6.10	289.16	5.91	4.17	H 015
0.0096	0.0009	0.0070	0.0050	290.70	6.18	299.79	14.08	9.08	H 7
0.0093	0.0008	0.0060	0.0100	275.03	3.50	285.79	3.03	10.76	H 8
0.0085	0.0021	0.0050	0.0020	262.22	5.37	271.01	2.14	8.79	H 3
0.0091	0.0020	0.0060	0.0110	286.00	4.39	291.50	12.71	5.50	H 5
0.0098	0.0009	0.0200	0.0060	273.50	3.86	288.50	3.46	15.00	H4
0.0091	0.0008	0.0190	0.0410	227.62	3.69	221.74	4.86	-5.88	H 6
0.0063	0.0009	0.0210	0.0090	273.33	9.42	273.65	8.01	0.33	H 13
0.0051	0.0019	0.0040	0.0060	217.78	3.32	223.90	9.98	6.12	H 11
0.0056	0.0020	0.0050	0.0250	223.42	5.64	228.16	5.92	4.74	H 12
0.0060	0.0018	0.0160	0.0340	237.32	4.25	240.78	4.71	3.46	H10
0.0066	0.0019	0.0170	0.0000	300.15	2.78	299.35	15.85	-0.80	H9
0.0053	0.0006	0.0050	0.0060	273.82	3.16	283.33	3.98	9.51	H16
0.0051	0.0005	0.0120	0.0130	290.81	1.46	295.35	2.81	4.54	H14
0.0089	0.0018	0.0220	0.0000	312.77	8.46	328.98	3.97	16.21	H01

In this data one can see that some heats exhibited age strengthening and some did not. The heats H002, H7, H8, H3, H4, H16, H14, and H01 showed age strengthening with 99 percent or higher confidence. Heat H6, where strength decreased by 6MPa during aging, was clearly not age strengthening and we can say with greater than ninety percent

confidence that H9 and H13 were not age strengthening and with 61 percent confidence that H02 was not age strengthening. Therefore the experiment has been successful in suppressing age strengthening and inducing age strengthening by varying the content of nitrogen, boron, aluminum and titanium in the same basis alloy. Detailed composition data is shown in Appendix 1.

DISCUSSION OF RESULTS

Since the chemical variables used presented some difficulty in reproducible alloy recovery, the traditional ANOVA approach presented a problem. The ANOVA approach assumes that we have only two values of each independent variable. However the alloying elements were in ranges. Near the latter portion of the matrix the researchers were able to improve the technique by inserting the envelopes under the melt quickly enough to avoid loss to slag layer entrapment.

Multiple variable regression correlation was used to get an initial picture of the relative importance of variables. It is important to note, as shown in Table 5, that the only compositional effect that increases age strengthening in this variable set appears to be nitrogen, although the confidence level is low at only 76 percent. Earlier work (Edington, Nicola, and Richards, 2002) indicated the importance of the nitrogen in limited sets of production iron. Iron heats from certain families of foundries where the nitrogen/titanium ratio was significantly different between heats showed some heats that exhibited age strengthening and others that did not. Also, the same authors found that the differential thermal analysis comparing irons that did not age strengthen to those that did showed evidence of the iron-nitrogen-carbon ternary eutectoid in the irons that showed age strengthening.

The multiple variable regression correlation approach was used to obtain an idea of the direction of influence and significance of the composition variables. The multiple variable regression results are shown in Table 6.

Table 5. Multiple Variable Regression Model of Statistical Effects of Variables

Variable	Coefficient	P-Value	Confidence
Nitrogen	+788	0.24	76%
Aluminum	-324	0.07	93%
Titanium	-173	0.09	91%
Boron	-390	0.24	76%
Constant	6.07	0.28	72%

The overall equation suggested by the correlations is:

UTS_{20}-UTS_0 = 6.07+788*%N-324*%Al-173*%Ti+390*%B

Where "UTS_{20}-UTS_0" is the change in ultimate tensile strength in units of MPa for aging 20 days.

THE EFFECT OF ELECTROPOSITIVE ELEMENTS ON NITROGEN AND TOTAL INTERSTITIALS

The elements other than nitrogen were selected for their tendency to react with nitrogen. The influence of the other composition variables may explain the reduced R^2 for titanium's effect compared to previous foundry data. (Eddington, Richards and Nicola, 2002). The influence of nitrogen on age strengthening in this data set is shown in Figure 1, where the R^2 is only 0.09, although the multiple variable correlation result in Table 5 shows a 76 percent confidence that nitrogen does increase age strengthening. The influence of nitrogen over the range tested was only 9 percent of the observed variation as indicated by the R^2.

If one examines the enthalpy of formation of the nitrides of titanium, aluminum and boron in the temperature range from 1000°K-1700°K, the Fact-Sage database (Bale, et al, 2003) gives:

BN : -250KJ/mole

AlN : -329 KJ/mole

TiN: -336±2KJ/mole

This suggests that titanium should be most successful at suppressing age-strengthening if it is related to nitrogen in solid solution, although aluminum should be close enough that solution activity coefficients could have an effect on which is predominant. Boron should be less effective based on thermodynamic considerations. Titanium tends to react with nitrogen and carbon in the liquid state as is evident from typical titanium carbonitride morphology, while aluminum is known to form nitrides in the solid state in wrought steel technology. Figure 2 shows that titanium in this data set tends to decrease the amount of age strengthening between zero days and 20 days of room temperature aging. The multivariable regression correlation result in Table 5 shows a 91 percent confidence that this is true. The R^2 suggests that titanium level accounted for 32 percent of the variation in this dataset.

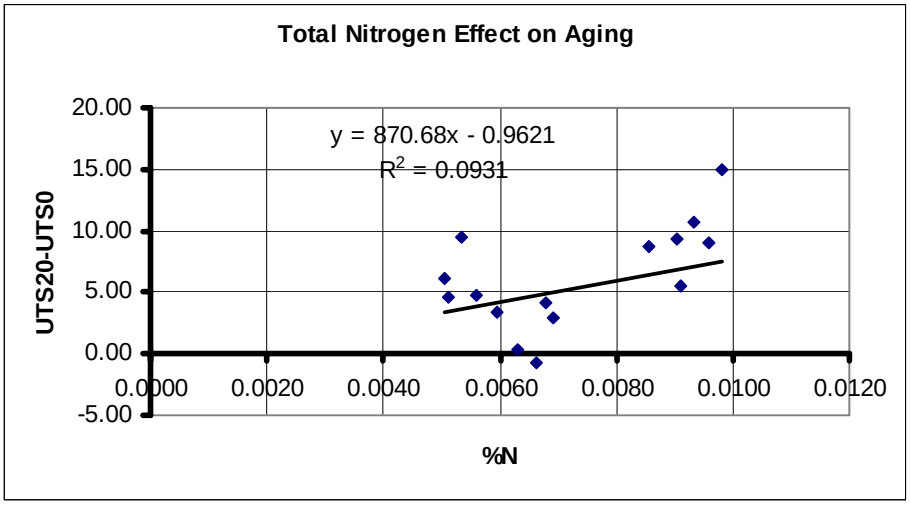

Figure 1 – The effect of nitrogen on age strengthening: Note that the vertical axis is the difference between the tensile strength within the first day and the tensile strength after 20 days natural aging

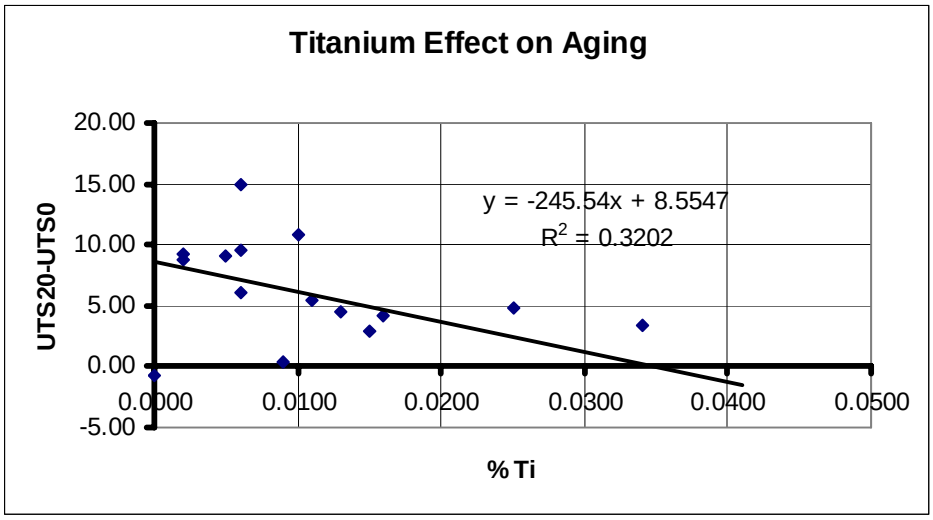

Figure 2 – The effect of titanium on age strengthening: this is the strongest variable in terms of correlation coefficient and agrees with previous work using foundry irons

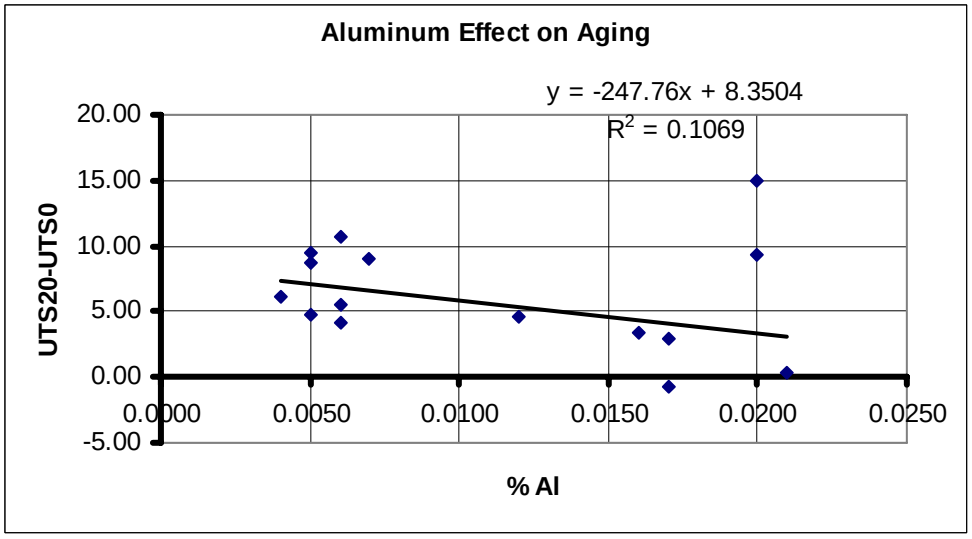

Figure 3 – The effect of aluminum in this data set is to suppress age strengthening

The trend of aluminum on suppressing age strengthening as indicated in Figure 3 is in agreement with anecdotal observations by some of the authors on production foundry irons that did not seem to exhibit age strengthening. The multiple variable correlation result suggests a 93 percent confidence level that this is true.

A similar analysis using a linear statistical model for boron indicates a weakly suppressing effect for age strengthening and that boron content only accounts for one percent of the effects on age strengthening in this data set. The multiple regression result did suggest a 76 percent confidence level that boron had suppressive influence on age strengthening. This result may be further refined with better boron analysis of the archived samples.

In terms of physical metallurgy, aluminum and titanium are relatively effective at removing interstitials from ferrite (carbon and nitrogen). Titanium carbo-nitrides are observable in gray iron microstructures with planar interfaces that reflect their crystal structure and suggest formation in contact with the liquid. If we correct the coefficients in the multiple regression model for the atomic weight ratio between the titanium and nitrogen and aluminum and nitrogen, we find that the corrected coefficients are closer, 623 for aluminum and 524 for titanium. However, the boron coefficient becomes significantly smaller.

Figure 4 shows an approximate relationship between the soluble nitrogen estimate used in earlier work and the change in strength upon aging. Based on atomic mass and 1:1 stoichiometry, the soluble nitrogen estimate is the nitrogen content minus one-third of the titanium content. The trend line shows an R^2 of 0.26 which is not as good as the data from the earlier work used by Eddington, Nicola, and Richards (2002). This is probably due to the variation of aluminum in the current dataset while in the cited paper the two foundries analyzed were both targeting a very limited range of aluminum values. Another confounding factor is that titanium also reacts with carbon and the reaction product is a mixed carbide-nitride solid solution.

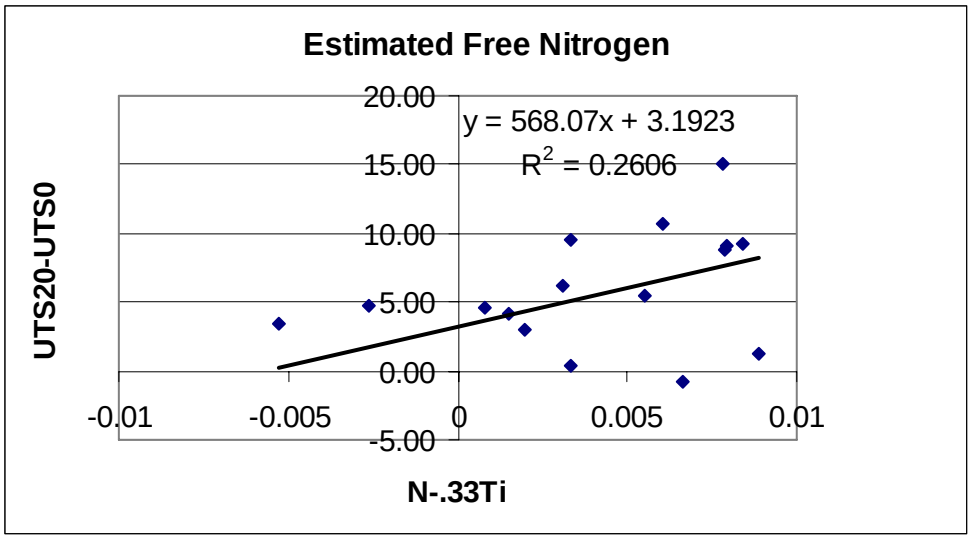

Figure 4 – Estimate of soluble nitrogen as a controlling variable for age-strengthening

A qualitative model of how these factors work together would assume that nitrogen and carbon in the ferrite are reacting to form a precipitate during the age-strengthening process. The titanium removes nitrogen from the iron during solidification and lowers the available nitrogen for solution in the ferrite. Aluminum may also remove some nitrogen during solidification and it may remove some as the casting cools through the austenite temperature range forming aluminum nitride or carbo-nitrides. The net effect of titanium and aluminum is to reduce the solubility of nitrogen in the ferrite and possibly the carbon solubility in ferrite. This leaves less reactant for the low temperature aging process.

CONCLUSION

The conclusions that one can draw immediately are:

1. Titanium and aluminum both strongly reduce age strengthening behavior.
2. Nitrogen tends to increase age strengthening.

Recommendations for further work would include:

1. Machinability effects of suppressing age strengthening behavior using aluminum.
2. Hot-Stage transmission electron microscopy studies of alloys that highly age strengthen.
3. Transmission electron microscopy of reaction product species involved in suppressing age strengthening.
4. Review boron effect after analysis of boron by ICP mass spectrometer.

Another area that may be of interest would be to examine alloying elements that have an influence on the kinetics – for example affecting the diffusivities of nitrogen and carbon. The objective would be chemically increasing the rate of aging to shorten aging times.

ACKNOWLEDGEMENT

The authors wish to acknowledge the support and guidance of the cosponsoring foundries and the guidance of the AFS 5H and 5I committees. The authors wish to recognize the contributions of undergraduate assistants who have worked on this project: Justin Novotny, Marilyn Emanuel, Sarah Taylor, William Cason, Ryan Spoering, and Allison Finch.

This paper is based on work supported by the U.S. Department of Energy under award number DE-FC36-04GO/4230 as subcontracted through Advanced Technology Institute. Any findings, opinions and conclusions or recommendations in this report are those of the authors and do not necessarily reflect the views of the Department of Energy.

REFERENCES

Bale, C. W., Pelton, A.D., Thompson, W.T., Eriksson, G., Hack, K., Chartrand, P., Degterov, S., Melancon, J., and Peterson S., Factsage 5.2, CRCT, Ecole Polytechnique, Montreal 2003

Edington, J, Nicola, W. M. and Richards, V., "Age Strengthening of Gray Cast Iron, Nitrogen Effects and Machinability", AFS Transactions, Volume 110, No: 2, pp 983-993 (2002)

Nicola, W. M. and Richards, V., "Age strengthening of Gray Cast Iron, Phase I: Statistical Verification", AFS Transactions, Volume 107, pp 749-756 (1999)

Nicola, W. M., and Richards, V., "Age Strengthening of Gray Cast Iron, Phase II: Nitrogen and Melting method effects", AFS Transactions, Volume 108, pp 233-237 (2000)

Nicola, W. M. and Richards, V., "Age Strengthening of Gray Cast Iron, Phase III: Effect of Aging temperature", AFS Transactions, Volume 109, pp 1085-1095 (2001)

Richards, V., Van Aken, David C., and Nicola, W.M., "Age Strengthening of Gray Cast Iron, Kinetics, Mechanical Property effects", AFS Transactions, Volume 111, paper 03-037, (2003)

Appendix 1 – Chemical analysis of 17 heats

# Heat	C%	Si%	Mn%	P%	Cu%	Cr%	N%	B%	Al%	Ti%	Day 1 UTS Ave. MPa	Day 20 UTS Ave. MPa
H 02	3.46	1.94	0.44	0.0560	0.3770	0.0890	0.0069	0.0021	0.0170	0.0150	259.06	262.00
H 002	3.49	1.93	0.36	0.0560	0.3710	0.0880	0.0091	0.0019	0.0200	0.0020	280.20	289.47
H 015	3.47	1.88	0.47	0.0540	0.3570	0.0900	0.0068	0.0087	0.0060	0.0160	285.00	289.16
H 7	3.43	2.11	0.41	0.0560	0.3780	0.0880	0.0096	0.0009	0.0070	0.0050	290.70	299.79
H 8	3.38	2.15	0.38	0.0550	0.3720	0.0870	0.0093	0.0008	0.0060	0.0100	275.03	285.79
H 3	3.37	2.13	0.40	0.0610	0.3510	0.0890	0.0085	0.0021	0.0050	0.0020	262.22	271.01
H 5	3.70	2.08	0.37	0.06	0.37	0.16	0.0091	0.0020	0.0060	0.0110	286.00	291.50
H4	3.41	2.17	0.37	0.0600	0.3190	0.0870	0.0098	0.0009	0.0200	0.0060	273.50	288.50
H 6	3.35	2.05	0.32	0.0580	0.3370	0.0870	0.0091	0.0008	0.0190	0.0410	227.62	221.74
H 13	3.34	1.94	0.43	0.0580	0.3420	0.0790	0.0063	0.0009	0.0210	0.0090	273.33	273.65
H 11	3.43	2.09	0.40	0.0530	0.3260	0.0830	0.0051	0.0019	0.0040	0.0060	217.78	223.90
H 12	3.32	2.10	0.45	0.0500	0.3200	0.0800	0.0056	0.0020	0.0050	0.0250	223.42	228.16
H10	3.39	2.08	0.41	0.0530	0.3240	0.0830	0.0060	0.0018	0.0160	0.0340	237.32	240.78
H9	3.37	1.97	0.37	0.0530	0.3120	0.0790	0.0066	0.0019	0.0170	0.0000	300.15	299.35
H16	3.42	2.12	0.45	0.0530	0.3400	0.0860	0.0053	0.0006	0.0050	0.0060	273.82	283.33
H14	3.28	1.96	0.39	0.0500	0.3100	0.0820	0.0051	0.0005	0.0120	0.0130	290.81	295.35
H01	3.33	2.09	0.34	0.0490	0.3200	0.0810	0.0089	0.0018	0.0220	0.0000	312.77	328.98

APPENDIX B

AGE STRENGTHENING OF GRAY IRON – KINETICS STUDY

Age Strengthening of Gray Iron – Kinetics Study

Von L. Richards, Thottathil V. Anish, Simon Lekakh, and David C. Van Aken
University of Missouri – Rolla
Wayne Nicola, Consultant, Warsaw, IN

ABSTRACT

Kinetics of gray cast iron strengthening at room and elevated temperature (100°C, 182°C and 285°C) were studied using 100 specimens cast from one industrial heat of gray iron. Tensile strength and Brinell hardness was measured during age strengthening. Peak aging was observed at shorter times for higher temperatures and over-aging was observed at 182°C and 285°C. Statistically significant data was used for evaluating aging kinetics and the determination of activation energies for precipitation. Tensile strength-temperature-time curves were described using Arrhenius and Avrami-Johnson-Mehl kinetics and an attempt was made to create a predictive model for age strengthening in gray iron. Earlier literature and a current study with another foundry indicate improvement of machinability with aging. The proposed model will help in optimizing the process for maximum tool life.

INTRODUCTION

This work is the result of AFS-CMC related research. The research is the continuation of previous work done by Nicola and Richards. Nicola and Richards (1999) demonstrated statistically that there is significant age strengthening in most gray cast iron alloys. The increase in tensile strength range from 3.3% to a high of 13.5%. The rate of increase follows an Avrami-Johnson-Mehl curve, so that much of the change occurs in the initial few days. Also, during this phase the excess nitrogen (the nitrogen in excess of the stoichometric amount to combine with *Ti* as *TiN*) was found to be an important factor. Nicola and Richards proposed that age strengthening was related to the interaction of nitrogen with dislocations. The diffusivity of nitrogen is significant at room temperature and could facilitate this mechanism. In Phase II of this study, Richards, Van Aken and Nicola (2000) verified that the presence of a strong nitride former (like *Ti*) can reduce the strengthening effect in iron, but did not fully eliminate the aging. The effect of nitrogen as a strength enhancer was confirmed in this research. The possibilities of precipitation of nitrides in the solid state and nitrogen in interstitial interaction with dislocations have been mentioned (Leslie , 1981). Another possibility that they noted is the development of titanium-nitrogen substitutional interstitial defect clusters, similar to that formed in steel (Leslie, 1981). These results in the hardening of iron based alloys containing nitrogen and titanium well in excess of the stoichometric amounts for the nitrogen. Richards et al (2000) indicated the presence of iron nitride and/or carbo-nitride forming as

the mechanism for aging. The presence of titanium does not appear to enhance or retard the age strengthening provided nitrogen is in excess to that required for stoichometric titanium nitride compound. Age strengthening is not observed when there is a large excess of titanium (Richards *et al.*, 2006)

It is important to note that improvements in machinability occur concurrently with the strengthening of gray iron. Various machining parameters were studied by Edington *et al*. (2002) and the results showed a sigmoidal relationship with the time of ageing (Figure 1). Also in the same year a neutron scattering study was conducted to determine the mechanism underlying aging. The scattering data revealed a resolved peak for the nitrogen rich gray iron sample at 28 days. This peak corresponded to a particle with a diameter 2-4nm or an ordered array of particles with interparticle spacing of 3.7nm. This size is similar in magnitude to the iron nitride clusters described by Edmonds and Honeycombe in 1978. But they did not have enough data to establish this fact since only one of the samples showed this behavior. In this described study, the role of free nitrogen in age strengthening was established by plotting the changes in UTS with log time. The age strengthening increased with increase in free nitrogen.

Later, through differential scanning calorimetry Richards *et al.,* (2003) established the strengthening phenomenon as a precipitation process which is reasonable in light of the Avrami-Johnson-Mehl transformation kinetics. Differential scanning calorimetry studies revealed two significant exothermic reactions in fully aged gray iron: one at 250°C and the other at 530°C. At 250°C transformation of metastable *Fe-N* to stable *Fe-N* happens and the second transformation is the ternary eutectoid transformation (Figure 2). Low temperature exothermic peak corresponds to the transformation of the metastable $Fe_{16}N_2$ *(α")* to the stable Fe_4N *(γ').* Furthermore the high temperature exothermic peak may be considered as the ternary eutectoid transformation *(α-Fe + Fe3C + γ'→ γ-Fe)* at 565°C. Also in this study, it was reported that hardness increased with time. All of the reported results are consistent with a quench aging phenomenon associated with free nitrogen in the iron.

Richards *et al.* (2006) showed the effect of various nitrogen getters on age strengthening. They concluded that *Ti* had a strong influence on arresting the age strengthening behavior. An estimate of interstitials could be predicted. Figure 3 illustrates the effect of increasing total interstitials in ferrite on the age strengthening in gray iron. In this work, the soluble nitrogen was estimated according equation (1)

$$\% \text{ soluble nitrogen} = \%N - 0.33\%Ti \qquad (1)$$

The goal of this study was evaluation of kinetics of iron strengthening at room and elevated temperatures for predicting and process design as well as shedding some light on the mechanism of age strengthening in gray irons.

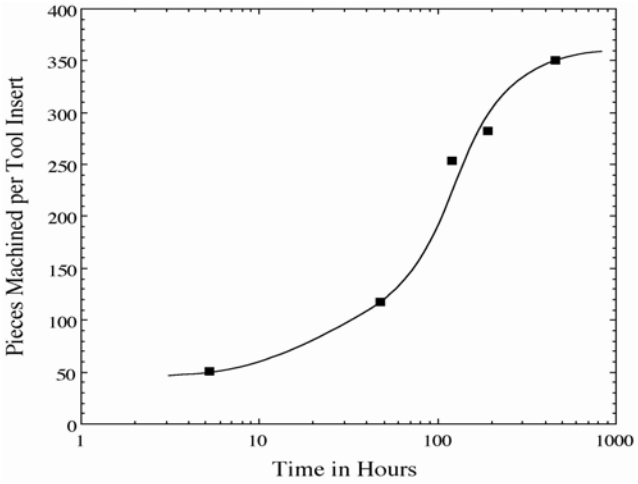

Figure 1. Effect of Aging on Machinability- Edington et al. (2002)

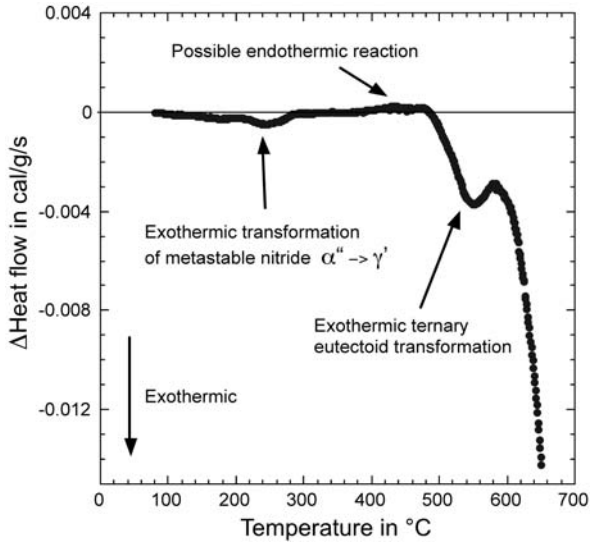

Figure 2. Differential scanning calorimetry results showing a difference curve generated by running a high nitrogen specimen in the reference cell and a non-aging specimen in the sample cell– Richards et al. (2003)

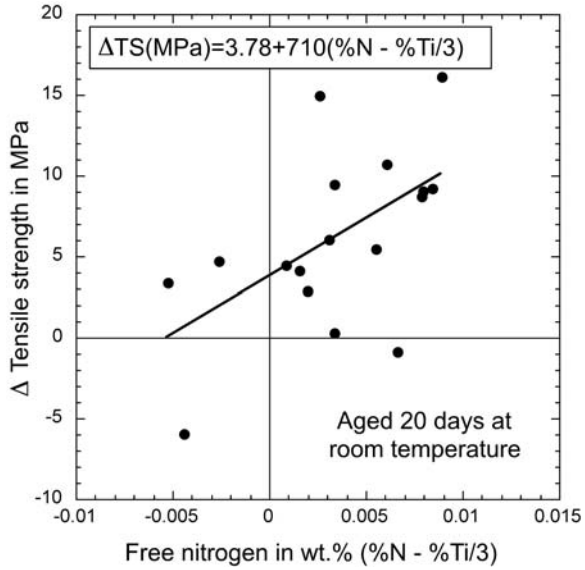

Figure 3. Estimate of soluble nitrogen as a controlling variable for age-strengthening - Richards et al. (2006)

EXPERIMENTAL PROCEDURE

DESIGN OF THE EXPERIMENT

The experimental conditions were designed based on published experimental data (Richards and Nicola, 2001) and kinetics based upon Johnson Mehl-Avrami kinetics. A generalized form of the Johnson-Mehl equation is shown as eq. (2)

$$V_f = 1 - \exp\left(\frac{-\pi}{3} J^r G^s t^{r+s}\right) \tag{2}$$

where V_f is the fraction transformed, J is the nucleation rate, G is the growth rate, t is the transformation time and r and s are exponents related to nucleation and growth. The Avrami equation, has also been used to describe phase transformations. Here the equation is written in a fashion such that the reaction rate constant k will always have units of reciprocal time.

$$V_f = 1 - \exp\left(-(kt)^n\right) \tag{3}$$

The rate constant k is defined by the following relationship

$$k = k_0 \exp\left(\frac{-Q}{RT}\right) \tag{4}$$

where R is the gas constant, T is the absolute temperature, k_0 is an attempt frequency and Q is the activation energy. If the time exponent n, k_0 and Q are constant over a range of temperatures, the reaction is said to be isokinetic in that temperature range.

The previously published results (Richards et al (2001), Edington *et al*. (2002)) showed that the age strengthening effect was a maximum after 15 days at room temperature aging, after 10 hours at 182°C and after 3 hours at 285°C. A time exponent of 4 was chosen for the solid state precipitation transformation (Cahn and Haasen, 1983), which assumes a constant nucleation rate (r=1) and a 3-dimensional growth of the precipitate (s=3). A value of JG^3 was determined for each temperature and the time (t) required to complete a particular fraction ($V_f(t)$) of the reaction was calculated. Calculated aging curves are shown in Figure 4 for room temperature, 182°C, and 285°C and these results were used to plan the age-hardening time interval for the cast iron used in this study. In addition, one set of bars was aged for longer periods of time to determine if the iron could be over-aged with subsequent loss of strength. The extended time was 11 hours at 285°C, 28 hours at 182°C, 37 hours at 100°C and 48 days at room temperature. The test parameter is shown in Table 1. Procedure of the samples randomization will be described below.

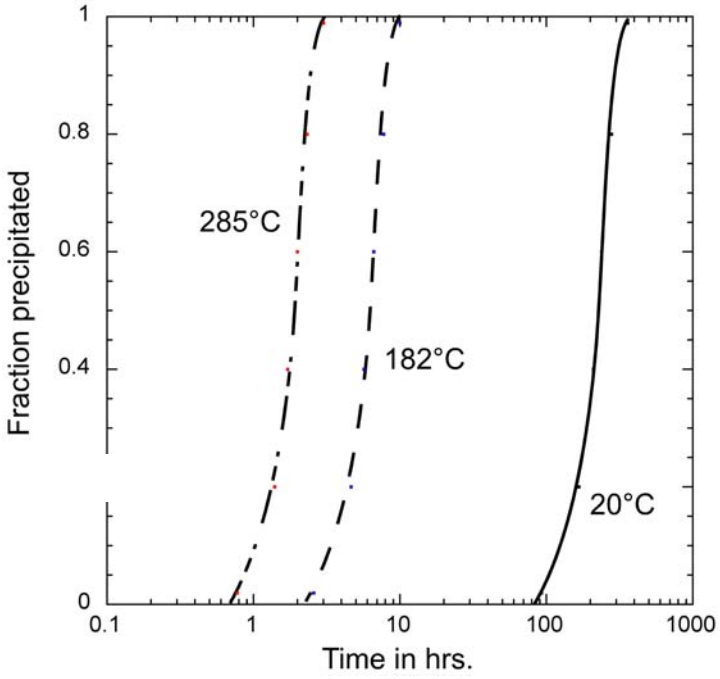

Figure 4. Forecast of aging kinetics with using Avrami-Johnson-Mehl equation

Table 1. Heat treatment time and temperature parameters

Temperature, °C	Aging time (hr)	Sample #	
Base	0	1	A
		23	A
		5	B
		26	A
		13	A
Base	0	16	A
		37	B
		12	B
		50	B
		16	B
Room T	4 day	18	B
		28	A
		50	A
		22	B
		20	A
Room T	6 day	45	B
		6	B
		4	B
		27	B
		31	B
Room T	9 day	38	A
		47	A
		19	B
		15	A
		40	B
Room T	15 day	21	A
		44	A
		45	A
		33	B
		13	B
Room T	19 day	8	B
		25	A
		43	B
Room T	25 day	34	A
		30	B
		49	B
Room T	46 day	32	A
		36	B
		37	A

Temperature, °C	Aging time (hr)	Sample #	
100	18.5	8	A
		6	A
		17	A
		48	B
		52	A
100	37	46	B
		42	A
		9	B
		38	B
		29	B
100	27	39	A
		48	A
		41	A
		34	B
		9	A
182	4	18	A
		51	B
		14	A
		36	A
		7	A
182	8	10	B
		47	B
		17	B
		24	B
		24	A
182	12	35	B
		3	A
		39	B
		23	B
		33	A
182	18	42	B
		15	B
		3	B
		31	A
		10	A
182	28	27	A
		30	A
		40	A
		12	A
		51	A

Temperature, °C	Aging time (hr)	Sample #	
285	0.75	44	B
		49	A
		35	A
		43	A
		11	A
285	1.5	21	B
		46	A
		2	B
		26	B
		25	B
285	2.5	29	A
		5	A
		2	A
		28	B
		1	B
285	5	14	B
		19	A
		52	B
		41	B
		4	A
285	11	20	B
		7	B
		11	B
		22	A
		32	B

MELT PROCEDURE AND SAMPLES PREPARATION

Test bars were poured in one of the participating foundries. The casting process and melt recipe of the participating foundry was followed with the exception that the nitrogen level in the iron was raised to 70-81ppm from 60ppm by ladle addition of ferromanganese with nitrogen *(Fe75%Mn5%N)* to enhance age strengthening. Two chill samples were poured, one before and one after pouring the molds. The samples were analyzed in an arc spectrometer for Si, Cr, Mn, Ti, Al, P, & Cu. The results (Table 2) were verified with two other arc spectrometers. Nitrogen was analyzed using a Leco TC500 inert gas fusion analyzer. Carbon and sulfur was analyzed using a Leco carbon-sulfur combustion analyzer. 50 molds having pressed ceramic filter and two vertically placed test bars were poured. The temperature of the melt in the ladle at the beginning of pour was 1468°C and at the end of pouring was 1366°C. The castings were cooled for 20 minutes in the mold before shake out, air cooled for 25 minutes to a temperature less than 120°C and quenched in water for 5 minutes. The castings were numbered chronologically and the two bars from each mold were

designated as A and B and placed in dry ice. Sets with 5 bars each were grouped using a statistically randomized distribution. Test bars produced were machined at room temperature under coolant flow in conformance to ASTM A48 & SAE J431 specifications using a CNC lathe. The time consumed for machining a bar was approximately 7 minutes. After machining the test bars were immediately placed in dry ice.

ARTIFICIAL AGING AND MECHANICAL TESTING

A convection oven with an internal air recirculating fan was used for the artificial aging heat treatments. In addition to the oven temperature controller, the temperature of the samples was verified using a dummy test bar with an axial hole drilled to the center of the gage length. With this test arrangement, the aging time was recorded from the time the temperature inside the bar reached ± 5°C of the required aging temperature. The variation of temperature during holding time was ± 1°C. Aging times and temperatures for each set of bars are listed in Table 1. After aging, the bars were covered in dry ice. Prior to mechanical testing, each bar was stabilized to room temperature in a water bath. Tensile tests were performed using a MTS Model 312.31 test frame with a 100 kN servohydraulic actuator and equipped with an Instron 8800 digital control and data acquisition system. Button-ended test specimens were held on the tapered shoulders in fully articulated box grips. Brinell hardness indentations were measured using an optical microscope equipped with a digital camera and a computer using Scion Image Analyzer. The calculated uncertainties in the reported measurements were based upon one sample standard deviation.

Table 2. Chemical analysis of iron

	Start pour	Finish pour
Temperature, ºC	1468	1366
C	3.46	3.44
Si	2.13	2.13
Mn	0.83	0.83
P	0.0840	0.0820
Cu	0.2900	0.2960
Cr	0.0770	0.0770
N	0.0081	0.0070
B	0..0080	0.0100
Al	0.0053	0.0052
Ti	0.0145	0.0147

RESULTS

Tensile strength data with calculated averages and uncertainties for the aging studies are shown in Figure 5. Brinell hardness measurements for these same irons are shown in Figure 6. The statistical evaluation of experimental data showed that aging did occur between the first and maximum strength data set with a 95% confidence level. Age strengthening was observed in both strength and Brinell hardness measurements at all the temperatures studied. Natural aging was observed after 20 days and reached what appeared to be a terminal value after 24 days. Close examination of the tensile strength and hardness data for the room temperature and 100°C aged iron shows a dip in the age strengthening response. This dip occurs just prior to the onset of significant age strengthening at room temperature and 100°C. Increasing temperature accelerated the age strengthening process and decreased peak aging times to 30-40 hours at 100 °C, 10-15 hours at 182°C, and finally, to only 4-6 hours at 285°C. Strength and hardness data for the elevated temperature aging studies show a continuous increase to a peak value. Increasing aging temperature from room temperature to 285°C also increased the maximum value of tensile strength. An over-aging effect was also discovered when the iron was aged at 182°C and 285°C where a loss in tensile strength was observed upon continued aging at temperature.

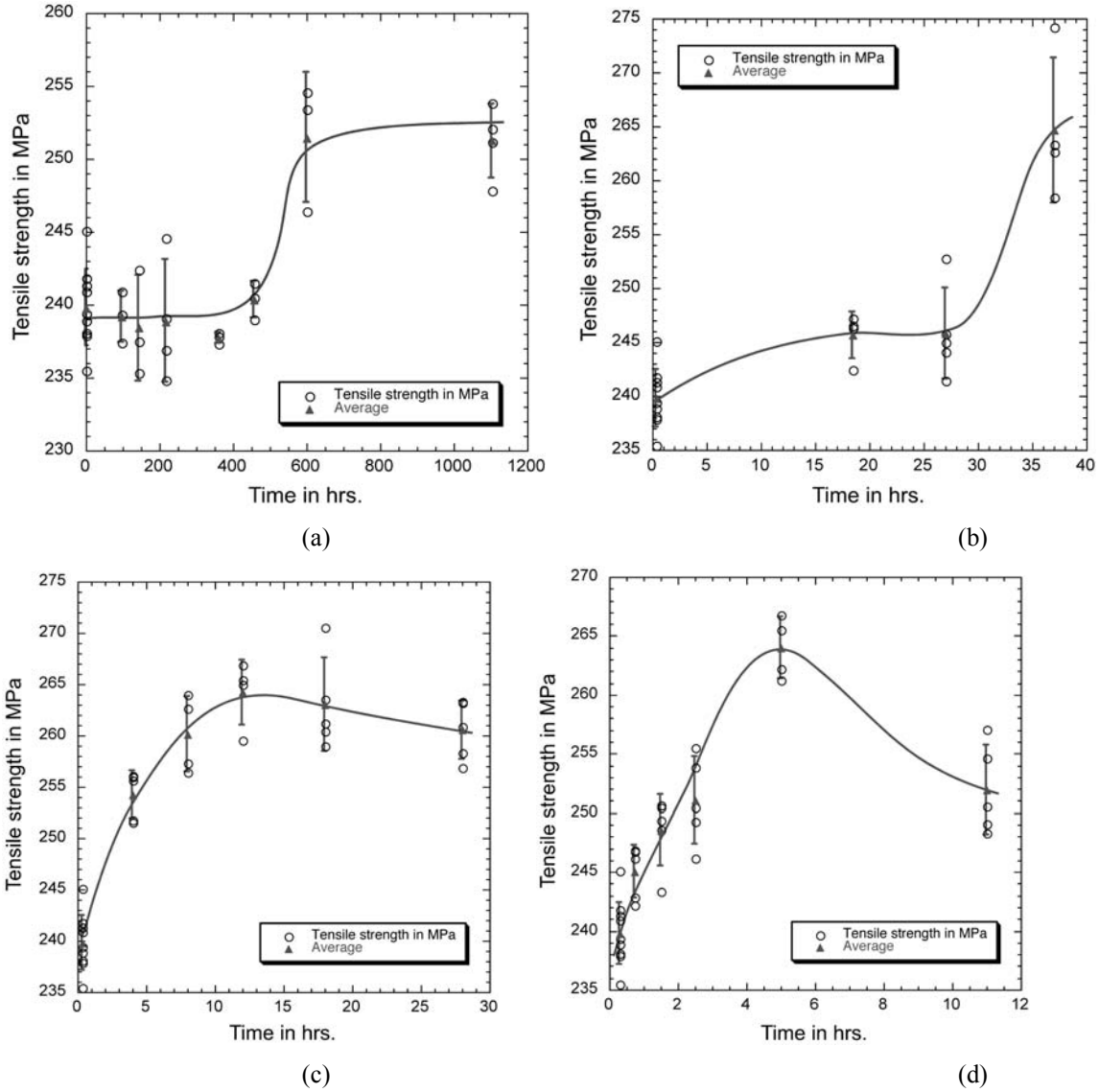

Figure 5. Tensile strength of iron during aging. (a) at room temperature (b) at 100°C (c) at 182°C and (d) at 285°C

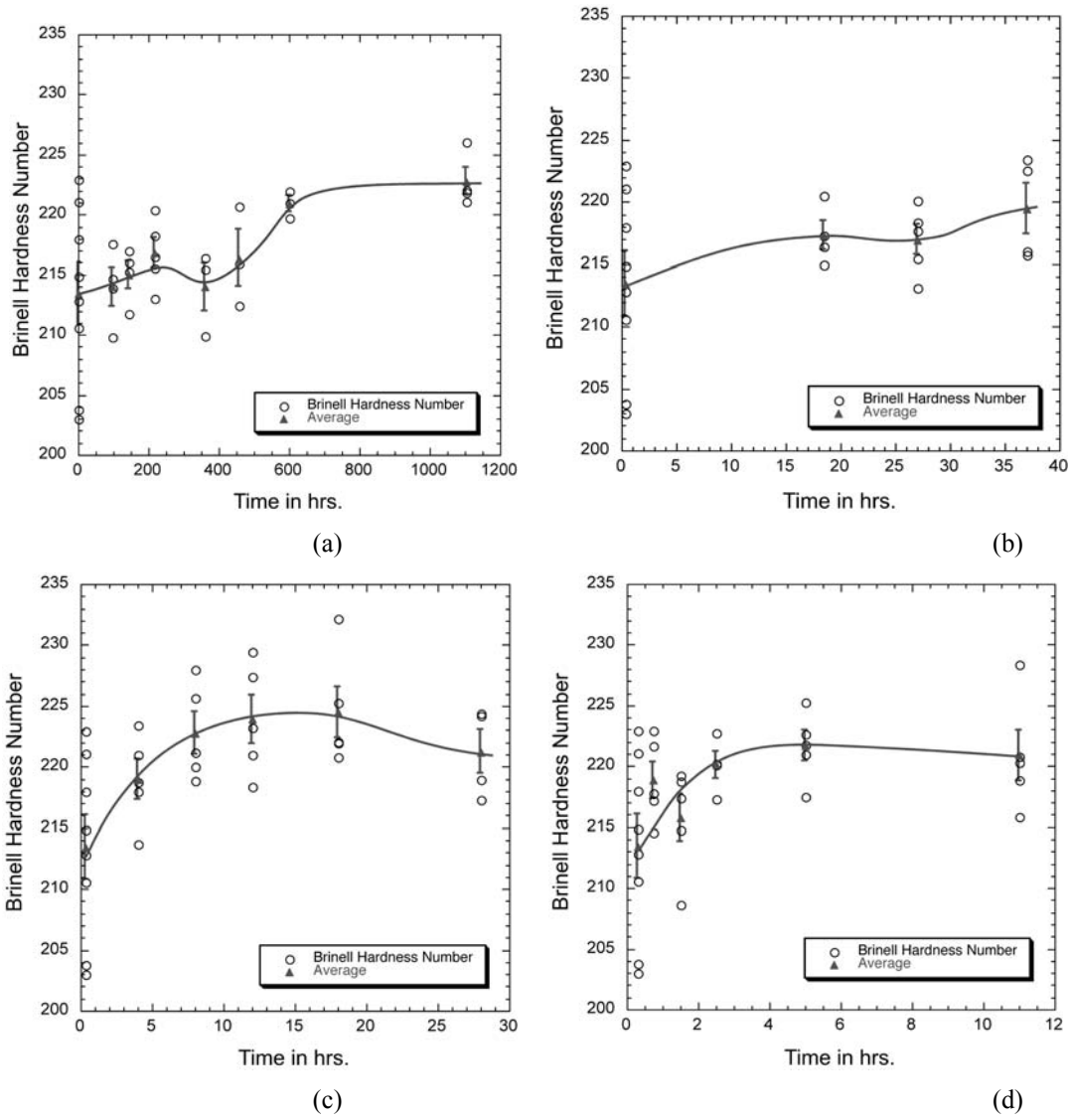

Figure 6. Brinell hardness of iron during aging. (a) at room temperature (b) at 100°C (c) at 182°C and (d) at 285°C

DISCUSSION OF RESULTS

KINETICS OF IRON AGING

Full natural aging was completed in 25 days which is significantly longer than the 15 days observed in previous studies (Richards et al 2001). The difference in aging kinetics could be explained by chemistry variations (see Table 3). The iron, which showed faster aging, had a higher concentration of soluble nitrogen, defined as a difference between total nitrogen content minus 0.33Ti and a lower manganese content. Manganese can significantly retard the nucleation of

nitrides in steel (Enrietto et al. 1962) by forming a substitutional and interstitial complex in the α-Fe. Thus, a combination of lower free nitrogen and higher manganese may have contributed to a slower room temperature age-hardening response in the current study. The Mn-N complexes are also known to interact with dislocations and produce strengthening. Thus, the loss in strength and hardness just prior to the onset of age strengthening may be related to the depletion of nitrogen from these Mn-N-dislocation complexes.

Table 3. Comparison of iron chemistry and aging time at room temperature

Parameters	Previous test (Richards, et al 2001)	Current study
Manganese, wt.%	0.51	0.80-0.83
Nitrogen, wt.%	0.0094	0.007-0.008
Aluminum, wt.%	0.003	0.005
Titanium, wt.%	0.012	0.014
Boron, wt.%	0.002	0.008
Soluble interstitial, wt.% (N – 0.33Ti)	0.0054	.0028
Natural aging time, days	15	28

Measured strength data was converted to a fraction precipitated, V_f, using the following relationship between the peak strength, S_{max}, the initial strength at $t = 0$, S_{min}, and the strength measured during aging, $S(t)$.

$$1 - V_f = \frac{S_{\max} - S(t)}{S_{\max} - S_{\min}} \tag{5}$$

Base samples and samples that over aged were removed from the analyses. The Avrami equation, eq. (3), was then used to evaluate the age strengthening kinetics of the iron (see Figure 7). Two distinct regimes are depicted in Figure 7 indicating that the age strengthening is not isokinetic over the temperature range investigated. At elevated temperatures (T>150°C) the time exponent, n, was determined to be 1.8 whereas the lower temperature data was fit by n=3.7. Rate constants were determined from Figure 7 where kt=1, which corresponds to an ordinate value of one in Figure 7.

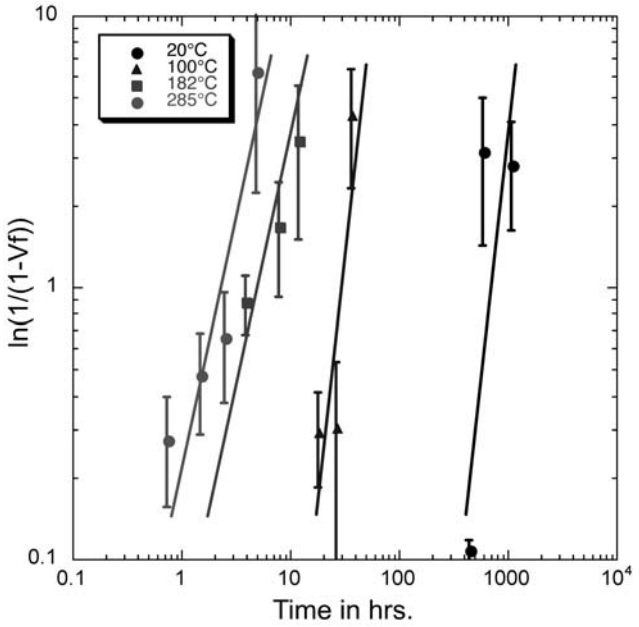

Figure 7. Age hardening data graphed assuming standard Avrami kinetics

An Arrhenius plot was constructed (see Figure 8) using the rate constants as determined above using coordinates of ln(k in hrs.$^{-1}$) versus the reciprocal of the absolute temperature (1/T(K)). An Activation energy, Q=16.8kJ/mole was determined for the 285 °C and 182 °C whereas Q= 35.7kJ/mole for the 100 °C and 20 °C data. Rasek(1983) reports an activation energy of 44kJ/mol for precipitation growth of nitrides in Fe-N system over the temperature range 50 to 180°C. It should be noted that activation energies determined using the Avrami relationship require considerable interpretation before a relationship to the diffusing species controlling the reaction rate is established.

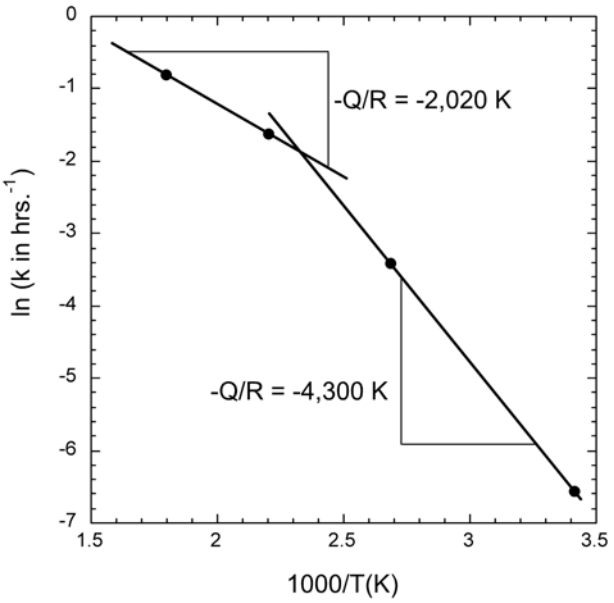

Figure 8. Arrhenius plot of iron aging kinetics

The activation energy Q may be written in terms of the activation energy for diffusion, q, the activation energy barrier to nucleation, ΔG^*, and the activation energy barrier to add an atom to the growing nucleus, $\Delta g^\ddagger$. Equation (6) is obtained by equating the exponential terms in the Johnson-Mehl equation for nucleation and growth with the exponential term in the rate constant k in the Avrami equation.

$$Q = \frac{r}{n} N_a \left(\Delta G^* + \Delta g^\ddagger\right) + \frac{s}{2n} q \qquad (6)$$

The expression above is for a transformation where a single new phase grows according to the parabolic growth law, where the growth velocity, G, is proportional to the diffusivity to the power 1/2 ($D^{1/2}$). In evaluating the various activation energies of this study, the transformation was assumed to be well below the solvus temperature of the precipitate. Thus, ΔG^* will be on the order of 10^{-19} J/ nucleus. For interstitials, $\Delta g^\ddagger$ was assumed to be zero, since interstitials do not occupy a lattice position in the parent phase and may be transported along the core of dislocations at the interface. Activation energies for diffusion (q) were then calculated for the different regimes and time exponents. For temperatures below 150°C, the time exponent was measured as 3.7 indicating a decreasing nucleation rate (r = 0.7) and spherical growth (s = 3) of the nucleus. An activation energy of 59.9kJ/mole was calculated for volume diffusion using eq. (6). The accepted value for nitrogen diffusion in α-Fe as measured by Wert (1950) is 76.1 kJ/mole.

At temperatures above 200°C, the nitrides are known to precipitate on dislocations and grow as disks with habit planes of $\{100\}_{\alpha\text{-Fe}}$ for α"- $Fe_{16}N_2$ or $\{210\}_{\alpha\text{-Fe}}$ for γ'-Fe_4N. Thus, the nucleation could be considered as site saturated (r = 0) where all of the nuclei exist at the beginning of the transformation. If we assume n=2 for the time exponent, which corresponds to growth of a disk-shaped particle (s = 2), a value of 33.6 kJ/mole is calculated for pipe diffusion of nitrogen along the dislocation core, which is approximately ½ the activation energy for lattice diffusion.

MECHANISM OF IRON AGING

Edmonds and Honeycombe (1978) provide a review of quench aging studies in Fe-N alloys that indicates a three stage precipitation process beginning with the formation of interstitial-atom clusters, followed by nucleation of α"- $Fe_{16}N_2$ and ending with equilibrium γ'-Fe_4N. Precipitation of α"- $Fe_{16}N_2$ can be nucleated homogeneously at low temperatures and high nitrogen supersaturations or heterogeneously on dislocations at higher temperatures and low nitrogen supersaturations. At temperatures above 200°C, the metastable α"- $Fe_{16}N_2$ is replaced by the ordered γ'-Fe_4N. It is proposed here that the same sequence occurs during age strengthening of gray irons. In this regard the neutron scattering studies reported by Edington et al. (2002) support evidence of interstitial atom clusters that are spherical in shape and the low temperature kinetic results reported in this paper support that conclusion where the time exponent suggest an equiax-shaped precipitate. The rate of cluster formation also appears to be affected by manganese concentration where high manganese concentrations may retard cluster formation. Furthermore, the apparent dip in strength and hardness data prior to the onset of age strengthening may be a result of dissociation of nitrogen from N-Mn-dislocation complexes and the initial stages of nitrogen cluster formation. Strength of these clusters would be proportional to the cluster radius and the cluster volume fraction to the power of ½ ($r^{1/2}P_f^{1/2}$), which assumes the cluster

is sheared by a moving dislocation. At longer aging times, α"- $Fe_{16}N_2$ precipitates on dislocations and depletes the clusters via pipe diffusion along dislocation cores. It should be anticipated that α"- $Fe_{16}N_2$ precipitation may be more homogeneous in irons with higher nitrogen supersaturations than that studied here. Aging temperatures of 182 °C and 285°C are most likely above the solvus temperature of α"- $Fe_{16}N_2$ for the irons studied here and heterogeneous precipitation of γ'-Fe_4N on dislocation would be anticipated. This conclusion is supported by the low value of activation energy and a time exponent that roughly agrees with the growth of a disk-shaped particle as expected for γ'-Fe_4N. Furthermore, the strength aging curves at 182°C and 285°C suggest a single precipitation event.

Modeling the low temperature age strengthening response in gray irons is complicated by the manganese effect; however, the results from this study suggests that irons can be formulated with low manganese and high nitrogen to obtain a quicker aging response. Heat treatment may also be an option and possibly less dependent upon manganese content. The following relationship is based upon the 182 °C and 285 °C aging kinetics observed in this study where the time to peak age, t_{peak}, is calculated in hours and temperature, T is the absolute temperature in Kelvin.

$$t_{peak} = 0.171 \exp \frac{2020}{T} \qquad (7)$$

Peak aging times of 14.5 hours and 6.4 hours are predicted for the aging temperatures of 182°C and 285°C using eq. (7). Complete understanding of age strengthening in gray irons will require further study and it should be cautioned that eq. (7) does not account for alloy chemistry, e.g. nitrogen and manganese, which may affect both the precipitate sequence and aging kinetics.

PRACTICAL SIGNIFICANCE

Referring to the paper by Edington *et al*. (2002) and Figure 1 it is clearly evident that machinability improves with aging. The kinetics study done in this paper shows that aging can be accelerated and equation 7 helps in calculating the time for maximum aging, t_{peak} , for a particular absolute temperature, T. It was found during this study that maximum strength can be attained significantly faster at a higher temperature as compared to normal room temperature aging. From the equation 7, we can predict that at 285°C, the maximum strength is attained in just 6.4hr compared to the room temperature time of 24-25days. Traditional method of storing the castings for several days before machining can be cut down to just few hours at a higher temperature resulting in savings in floor space and inventory costs.

CONCLUSION

The current study revealed that the age strengthening phenomenon in gray iron is not limited to a single mechanism at all temperatures and that over aging is possible. Full strength can be achieved in as little as 4-6 hours at 285°C. Approximate activation energy values have been obtained that show the aging process is most likely associated with nitrogen clusters at low temperatures and nitride precipitation at elevated temperature. A predictive model for the time

to peak age was formulated based upon the elevated temperature aging study and may be useful in planning accelerated aging processes at temperatures between 150°C and 300°C.

Future work should focus on alloy chemistry and the effect of manganese content on age strengthening. This study also indicates that difficulty in observing microstructural changes via transmission electron microscopy may be related to the cluster nature of the precipitates and future work will examine the 182°C and 285°C aged specimens from this study.

ACKNOWLEDGEMENT

The authors wish to acknowledge the support and guidance of the cosponsoring foundries and the guidance of the AFS 5H and 5I committees. The authors wish to recognize the contributions of undergraduate assistant who has worked on this project: Megan McGrath.

This paper is based on work supported by the U.S. Department of Energy under award number DE-FC36-04GO/4230 as subcontracted through Advanced Technology Institute. Any findings, opinions and conclusions or recommendations in this report are those of the authors and do not necessarily reflect the views of the Department of Energy.

REFERENCES

Bale, C. W., Pelton, A.D., Thompson, W.T., Eriksson, G., Hack, K., Chartrand, P., Degterov, S., Melancon, J., and Peterson S., Factsage 5.2, CRCT, Ecole Polytechnique, Montreal 2003

Cahn R.W. and Haasen P., Physical Metallurgy, Part 2, p.988, Elsevier Science Publisher, 1983

Edington, J, Nicola, W. M. and Richards, V., "Age Strengthening of Gray Cast Iron, Nitrogen Effects and Machinability", AFS Transactions, Volume 110, No: 2, pp 983-993 (2002)

Edmonds, D.V., and Honeycombe, R.W.K., "Precipitation in Iron-base Alloys," in Precipitation Processes in Solids, eds. K.C. Russell and H.I. Aaronson, The Metallurgical Society of AIME (1978)

Enrietto, J.F., Wells, M.G.H., and Morgan, E.R., "Quench aging in Fe-Mn-C-N Alloys" in Precipitation from Iron-base Alloys, Metallurgical Society Conf. Vol. 28, eds. G.R. Speich and J.B. Clark, Gordon and Breach Science Publishers (1965)

Leslie, W. C., The physical metallurgy of steels, Tech book publications, pp. 32-55 (1981)

Nicola, W M and Richards, V, "Age strengthening of Gray Cast Iron, Phase I: Statistical Verification", AFS Transactions, Volume 107, pp. 749-756 (1999)

Nicola, W. M., and Richards, V., "Age Strengthening of Gray Cast Iron, Phase II: Nitrogen and Melting method effects", AFS Transactions, Volume 108, pp. 233-237 (2000)

Nicola, W. M., and Richards, V., "Age Strengthening of Gray Cast Iron, Phase III: Effect of Aging temperature", AFS Transactions, Volume 109, pp 1085-1095 (2001)

Rasek, Jozef. Activation energies of nitrogen diffusion, nitrides precipitation and resolution in alpha -iron-nitrogen. Diffusion and Defect Monograph Series, 7, pp 442-5. (1983)

Richards, V., Van Aken, David C., and Nicola, W.M., "Age Strengthening of Gray Cast Iron, Kinetics, Mechanical Property effects", AFS Transactions, Volume 111, paper 03-037, (2003)

Richards, V., Thottathil, V. Anish, Lekakh, S. and Van Aken, David C, "Composition Effects on Age Strengthening of Gray Iron" AFS Transactions, Volume 114, paper 06-047, (2006)

Wert, C. J., "Measurements on the Diffusion of Interstitial Atoms in bcc Lattices," Appl. Phys., Volume 21, p.1196 (1950)

BIBLIOGRAPHY

[1] Ebner, R, Giesserei 50, Nr 22, pp 689-691(1963)

[2] Nicola, W M and Richards, V, "Age strengthening of Gray Cast Iron, Phase I: Statistical Verification", AFS Transactions, Volume 107, pp. 749-756 (1999)

[3] Leslie W C The physical metallurgy of steels, Mc graw hill, , pp 89-91,(1981)

[4] Nicola, W. M., and Richards, V., "Age Strengthening of Gray Cast Iron, Phase II: Nitrogen and Melting method effects", AFS Transactions, Volume 108, pp. 233-237 (2000)

[5] Edington, J, Nicola, W. M. and Richards, V., "Age Strengthening of Gray Cast Iron, Nitrogen Effects and Machinability", AFS Transactions, Volume 110, No: 2, pp 983-993 (2002)

[6] Edmonds, D.V., and Honeycombe, R.W.K., "Precipitation in Iron-base Alloys," in Precipitation Processes in Solids, eds. K.C. Russell and H.I. Aaronson, The Metallurgical Society of AIME (1978)

[7] Richards, V., Van Aken, David C., and Nicola, W.M., "Age Strengthening of Gray Cast Iron, Kinetics, Mechanical Property effects", AFS Transactions, Volume 111, paper 03-037, (2003)

[8] Avner, S H, Introduction to Physical Metallurgy, Tata McGraw Hill Edition, pp 190-94, (1997)

[9] Baird, J D and Jamieson A, "High-temperature tensile properties of some synthesized iron alloys containing molybdenum and chromium". Journal of the Iron and Steel Institute, 210, 841-6, (1972)

[10] Malinov, S, Bottger, A J, Mittemeijer, E J, Pekelharing, M I, and Somers M A J, "Phase transformations and Phase equilibria in the Fe-N system at temperatures below 573K", Metallurgical and Materials transactions, Volume 32A, Jan – pp 59-73, (2001)

[11] Karin Frisk, "A New Assessment of the Fe-N Phase Diagram", CALPHAD, Vol 11, No. 2, pp 127-134, (1987)

[12] Burgess, P B, "Age hardening Ferritic Malleable Iron", AFS transactions, pp172-179, (1968)

[13] Wada, H, and Pehlke, R D , "Nitride formation in Solid cast irons" AFS transactions, Vol 73-69, pp 482-492, (1973)

[14] Glodowski, R.J, "Nitrogen Strain Aging in Ferritic Steels", Wire journal international, Vol. 38, pp 72-5, (2005)

[15] Wilson, F. G. and Gladman, T, "Aluminum nitride in Steel", International Materials Review, Vol. 33, No. 5, pp. 221-285, (1988)

[16] Fountain, R W and Chipman, John "Solubility and Precipitation of boron nitride in Iron-Boron alloys", Transactions of the Metallurgical society of AIME, Vol 224, pp 599-605 (1962)

[17] Evans, E R, "Nitrogen in Cast Iron – and its neutralization by Aluminum", BCIRA journal, Vol 17, pp 62-71 (1969)

[18] Uda M and Pehlke R D, "Solubility of nitrogen in liquid Fe-C-Si Alloys" , Cast Metals Research Journal, 10(1), pp 30-8, (1974)

[19] Nicola, W. M., and Richards, V., "Age Strengthening of Gray Cast Iron, Phase III: Effect of Aging temperature", AFS Transactions, Volume 109, pp 1085-1095 (2001)

[20] Cahn R.W. and Haasen P., Physical Metallurgy, Part 2, p.988, Elsevier Science Publisher, (1983)

[21] Bale, C. W., Pelton, A.D., Thompson, W.T., Eriksson, G., Hack, K., Chartrand, P., Degterov, S., Melancon, J., and Peterson S., Factsage 5.2, CRCT, Ecole Polytechnique, Montreal 2003

[22] FACTSage, CRCT, Ecole Polytechnique, Montreal, Canada

[23] Enrietto, J.F., Wells, M.G.H., and Morgan, E.R., "Quench aging in Fe-Mn-C-N Alloys" in Precipitation from Iron-base Alloys, Metallurgical Society Conf. Vol. 28, eds. G.R. Speich and J.B. Clark, Gordon and Breach Science Publishers (1965)

[24] Rasek, Jozef. Activation energies of nitrogen diffusion, nitrides precipitation and resolution in alpha - iron-nitrogen. Diffusion and Defect Monograph Series, 7, pp 442-5. (1983)

[25] Wert, C. J., "Measurements on the Diffusion of Interstitial Atoms in bcc Lattices," Appl. Phys., Volume 21, p.1196 (1950)

VITA

Thottathil Viswanathan Anish was born in Kerala, India on January 22, 1980. He received his primary education at Don Bosco High school in Kerala, India. In May 2001, he received his Bachelor of Engineering in Metallurgical Engineering from VNIT, Nagpur, India. After which he worked for almost four years in Tata Motors India Ltd, Pune, India as senior projects engineer. He received his Master of Science in Metallurgical Engineering at the University of Missouri-Rolla in May 2007. He has been a Graduate Research Assistant in the Department of Metallurgical Engineering, University of Missouri-Rolla from May 2005 until May 2007. He was a Graduate Teaching Assistant in the Department of Metallurgical Engineering, University of Missouri-Rolla from August 2005 until May 2005. He is also a student member of the American Foundry Society.